FUNDAMENTAL PHYSICS WITH LARGE/MEDIUM/SMALL SCALE STRUCTURES

LECTURE 3

Matteo Viel - SISSA

2022 Winter School

Tenerife (Spain)

Euclid Flagship Simulation

SISSA

PLAN

INTRO

FUNDAMENTAL PHYSICAL TESTS "BEFORE" GALAXIES ARE FORMED IN THE POST-REIONIZATION UNIVERSE

IGM
INTENSITY MAPPING

GALAXY CLUSTERING: DYNAMICAL AND GEOMETRICAL PROBE

WEAK LENSING

GALAXY CLUSTERS

CONNECTIONS

FABIO FINELLI: CMB x LSS

KFIR BLUM: SMALLER SCALES PROPERTIES OF GALAXIES

LUCA AMENDOLA: MODIFICATION OF GRAVITY/DARK ENERGY

OLGA MENA: NEUTRINOS

TRACY SLATYER: DARK MATTER

GALAXY CLUSTERING

Baumann et al. 2012 EFT of the LSS

Philcox & Ivanov 2021 - Full Shape power spectrum analysis

Manzotti, Peloso, Pietroni, MV, Villaescusa-Navarro 14 - Coarse Grained perturbation theory

Galaxy Formation and Evolution - Mo, Van Den Bosch & White book

DESI Collaboration (2016), arXiv:1611.00037

Alam et al. 2020 - full analysis of BOSS galaxy clustering

Semenaite+22, arXiv: 2210.07304 - Beyond LCDM with galaxies

Chapman+21 - Growth with galaxy clustering

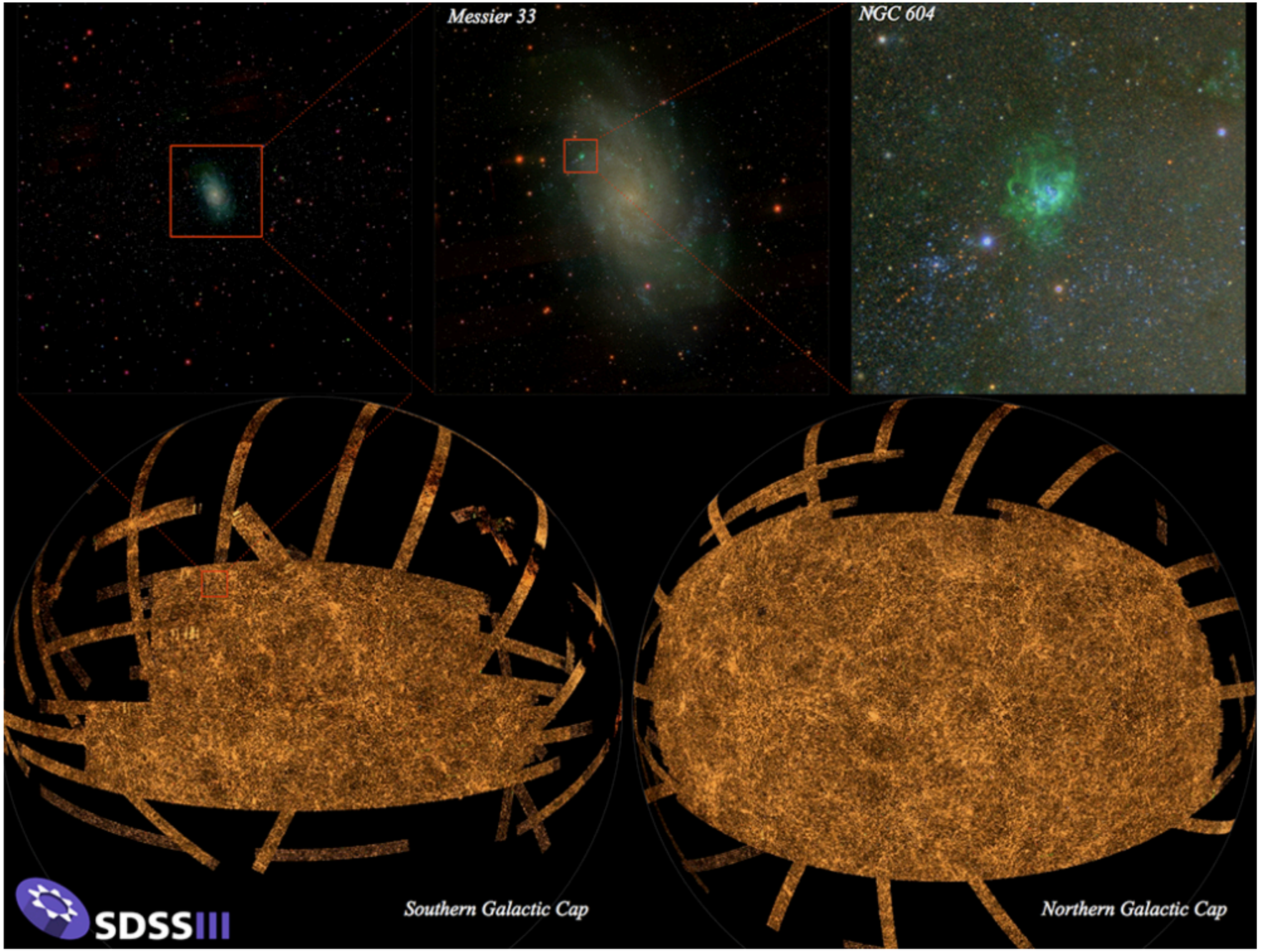
Messier 33
NGC 604
Southern Galactic Cap
Northern Galactic Cap
SDSSIII

The Sloan Digital Sky Survey

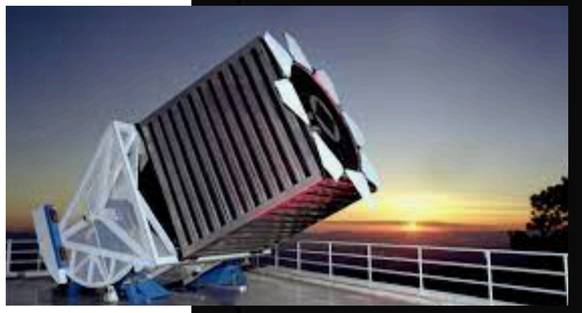

Cosmology from galaxy surveys

[from Will Percival]

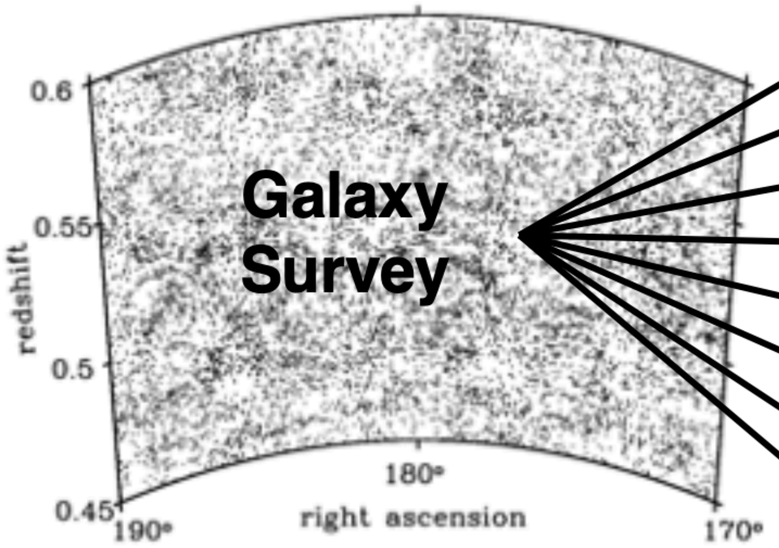

Matter and baryon density → Recombination power spectrum

Distance-redshift relation → Angular projected clustering scale (BAO & voids)

Hubble parameter → Radial projected clustering scale (BAO & voids)

Matter velocity power spectrum → Line-of-sight dependent clustering strength affected by RSD

Neutrino masses
Primordial non-Gaussianity → Small-scale damping of power
Varying growth of structure

Small-scale effects → Large-scale clustering for biased galaxy population / bispectrum

Isotropy / homogeneity → +Bispectrum, +small-scale MG, + galaxy properties, +…

Clustering as a function of position

Galaxies biased tracers of the underlying density field

Galaxy Clustering: Basics - I

Statistical description of galaxy distribution should shed light on underlying density field

$$\xi(x) = \langle \delta_1 \delta_2 \rangle$$

$$\xi(x) = \frac{1}{V_u} \sum_{\mathbf{k}} P(k) e^{i\mathbf{k}\cdot\mathbf{x}} = \frac{1}{(2\pi)^3} \int P(k) e^{i\mathbf{k}\cdot\mathbf{x}} \, \mathrm{d}^3\mathbf{k},$$

$$P(k) = V_u \langle |\delta_{\mathbf{k}}|^2 \rangle$$

$$\left\langle p^{(1)}(\mathbf{x}_i) p^{(1)}(\mathbf{x}_i + \mathbf{x}) \right\rangle_{\mathbf{x}_i} = (\bar{n} \Delta V)^2 [1 + \xi(x)]$$

$$\mathrm{d}N(r) = 4\pi r^2 \bar{n} [1 + \xi(r)] \, \mathrm{d}r,$$

Number of neighbours

"Mean density profile" around each particle

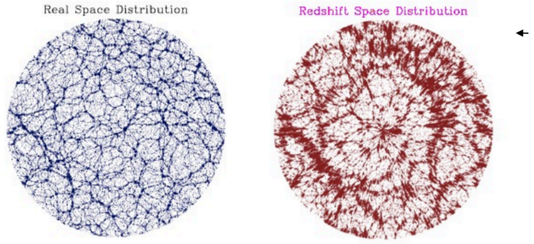

https://feldman.ku.edu/

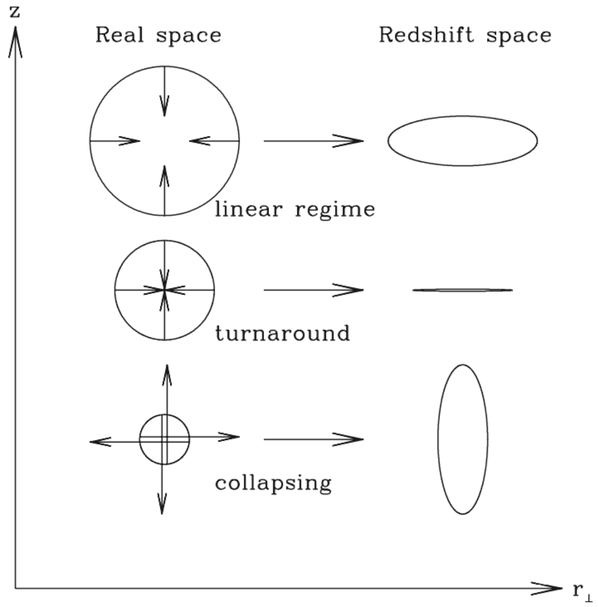

Galaxy Clustering: Basics - II

Redshift space breaks the isotropy but can be used for constraining cosmological models

In linear theory....

$$\beta \equiv f(\Omega_{\rm m})/b$$

$$\delta^{(s)}(\mathbf{r}) = \left[1+\beta\left(\frac{\partial^2}{\partial r^2}+\frac{2}{r}\frac{\partial}{\partial r}\right)\nabla_{\mathbf{r}}^{-2}\right]\delta(\mathbf{r})$$

$$\delta_{\mathbf{k}}^{(s)} = \left(1+\beta\mu_{\mathbf{k}}^2\right)\delta_{\mathbf{k}}, \quad \text{where} \quad \mu_{\mathbf{k}} \equiv k_z/k.$$

Plane-parallel approximation

$$P^{(s)}(\mathbf{k}) = \sum_\ell \mathscr{P}_\ell(\mu_{\mathbf{k}})P_\ell^{(s)}(k), \quad P_\ell^{(s)}(k) = \frac{2\ell+1}{2}\int_{-1}^{1} P^{(s)}(\mathbf{k})\mathscr{P}_\ell(\mu_{\mathbf{k}})\,\mathrm{d}\mu_{\mathbf{k}},$$

Linear large-scale model for power spectrum
(Kaiser 1987, MNRAS 227)

$$P^s(\mathbf{k}) = (b+f\mu^2)^2 P(k)$$

Redshift-space power spectrum

Linear deterministic local bias

RSD term depends on $f\sigma_8$

$$P_0^{(s)}(k) \equiv \left(1+\frac{2}{3}\beta+\frac{1}{5}\beta^2\right)P(k)$$

$$P_2^{(s)}(k) = \left(\frac{4}{3}\beta+\frac{4}{7}\beta^2\right)P(k), \quad P_4^{(s)}(k) = \frac{8}{35}\beta^2 P(k).$$

Angular correlation function, projected correlation function, evolution of correlation function etc.

Galaxy Clustering: Basics - III

But galaxies cannot be treated just like points

Selection effects: magnitude limited sample and/or volume limited sample

.... galaxy bias $$b(k) = b_{\rm lin}\sqrt{\frac{1+Qk^2}{1+Ak}}$$

On top of that window function not really easy to deal with

Peacock 1997 - Optical galaxies

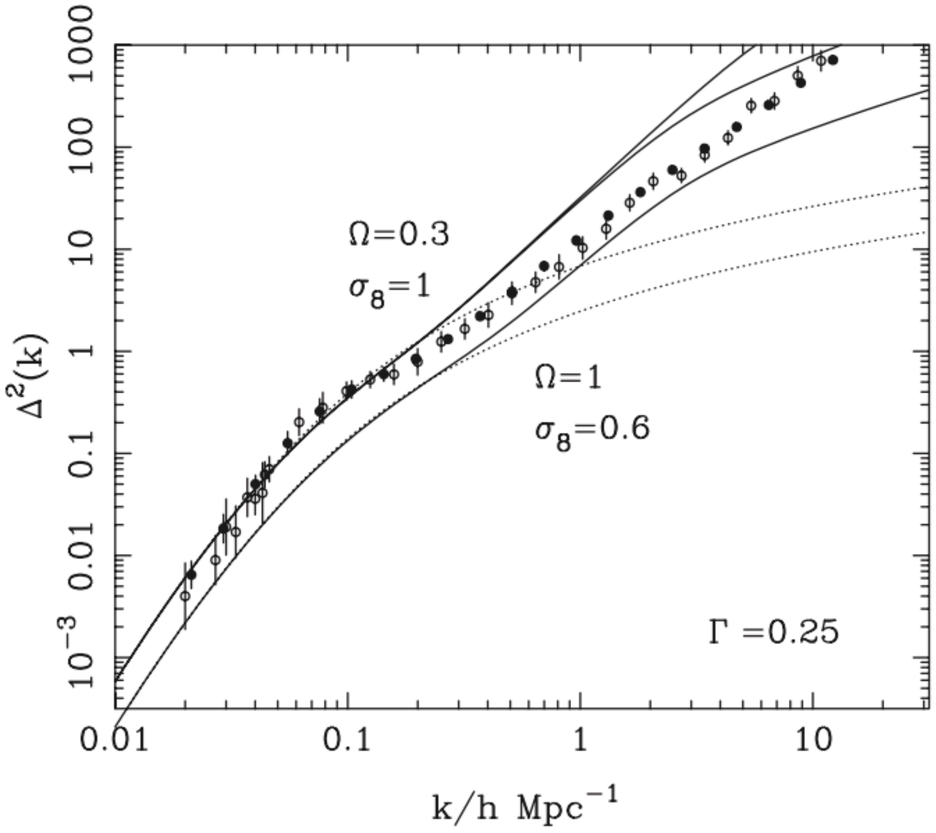

Cresswell & Percival 2009

Bin	Absolute magnitude range	Mean $M_{0.1_r}$	Galaxy count
Red 1	$-22.30 \leq M_{0.1_r} < -21.35$	-21.79 ± 0.27	49 167
Red 2	$-21.35 \leq M_{0.1_r} < -20.89$	-21.12 ± 0.13	41 462
Red 3	$-20.89 \leq M_{0.1_r} < -20.47$	-20.70 ± 0.12	37 819
Red 4	$-20.47 \leq M_{0.1_r} < -20.00$	-20.27 ± 0.14	34 651
Red 5	$-20.00 \leq M_{0.1_r} < -19.34$	-19.75 ± 0.19	29 742
Red 6	$-19.34 \leq M_{0.1_r} < -17.00$	-19.01 ± 0.38	17 582
Blue 1	$-22.30 \leq M_{0.1_r} < -21.35$	-21.67 ± 0.24	17 480
Blue 2	$-21.35 \leq M_{0.1_r} < -20.89$	-21.22 ± 0.13	25 208
Blue 3	$-20.89 \leq M_{0.1_r} < -20.47$	-20.69 ± 0.12	28 928
Blue 4	$-20.47 \leq M_{0.1_r} < -20.00$	-20.27 ± 0.14	32 066
Blue 5	$-20.00 \leq M_{0.1_r} < -19.34$	-19.74 ± 0.19	36 889
Blue 6	$-19.34 \leq M_{0.1_r} < -17.00$	-18.91 ± 0.49	48 754

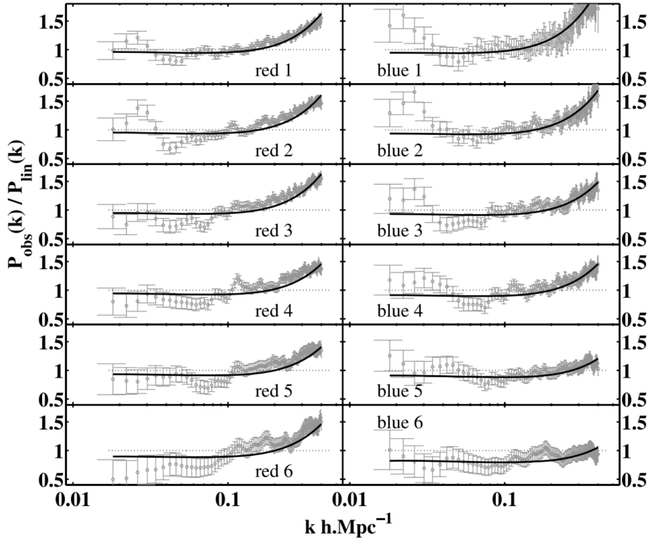

Galaxy Clustering: Basics - IV

Galaxy (Halo) bias

Number of haloes

$$N(1|0)\,\mathrm{d}M_1 = \frac{M_0}{M_1} f(1|0) \left|\frac{\mathrm{d}S_1}{\mathrm{d}M_1}\right| \mathrm{d}M_1,$$

M0 could be halo
mass or mass of a Lagrangian region (not collapsed)

$$f(1|0)\,\mathrm{d}S_1 \equiv \frac{1}{\sqrt{2\pi}} \frac{\delta_1 - \delta_0}{(S_1 - S_0)^{3/2}} \exp\left[-\frac{(\delta_1 - \delta_0)^2}{2\,(S_1 - S_0)}\right] \mathrm{d}S_1.$$

$$\delta_{\rm h}^{\rm L}(1|0) = \frac{N(1|0)}{n(M_1, z_1) V_{\rm L}} - 1, \quad \text{where} \quad V_{\rm L} \equiv \frac{4\pi}{3} R_0^3.$$

$$\delta_{\rm h}^{\rm L}(1|0) = \frac{\nu_1^2 - 1}{\delta_1} \delta_0, \quad \text{where} \quad \nu_1 = \frac{\delta_1}{\sqrt{S_1}}.$$

$$\delta_{\rm h}(1|0) = \frac{N(1|0)}{n(M_1, z_1) V_{\rm L}} \frac{V_{\rm L}}{V_{\rm E}} - 1, \qquad V_{\rm L}/V_{\rm E} = 1 + \delta(t).$$

$$\delta_{\rm h}(1|0) = \delta(t) + \frac{\nu_1^2 - 1}{\delta_1} \delta_0 + \frac{\nu_1^2 - 1}{\delta_1} \delta_0 \delta(t)$$

$$\delta_{\rm h}(1|0) = b_{\rm h}(M_1, \delta_1; t)\, \delta(t),$$

$$b_{\rm h}(M_1, \delta_1; t) = 1 + \frac{1}{D(t)} \left(\frac{\nu_1^2 - 1}{\delta_1}\right)$$

Simple (linear) bias model

Galaxy Clustering: Assembly bias - I

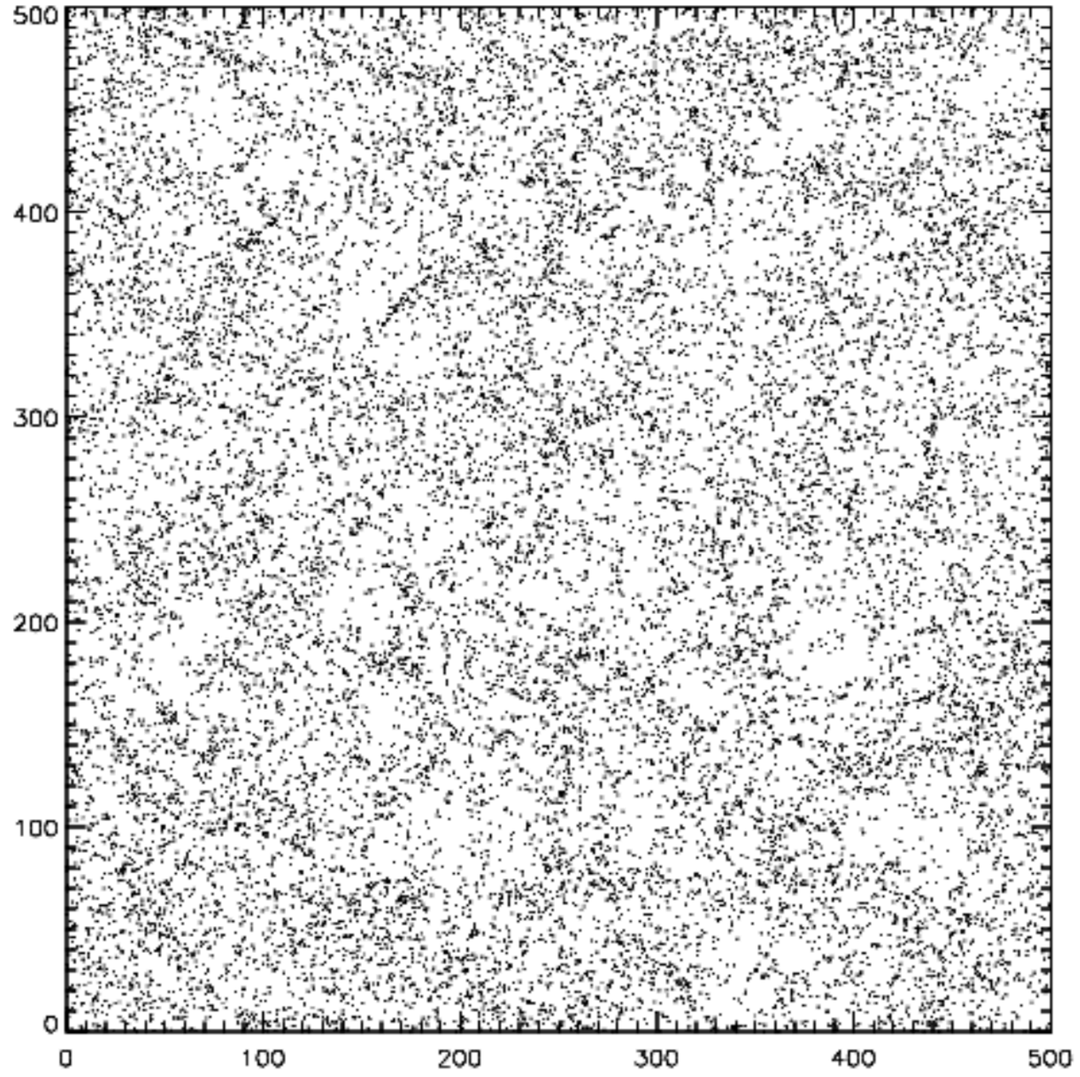

Gao, Springel & White 2005

The 20% of halos with the *latest* half-mass assembly redshifts in a 30 Mpc/h thick slice

$$M_{halo} \sim 10^{11} M_{\odot}$$

Galaxy Clustering: Assembly bias - II

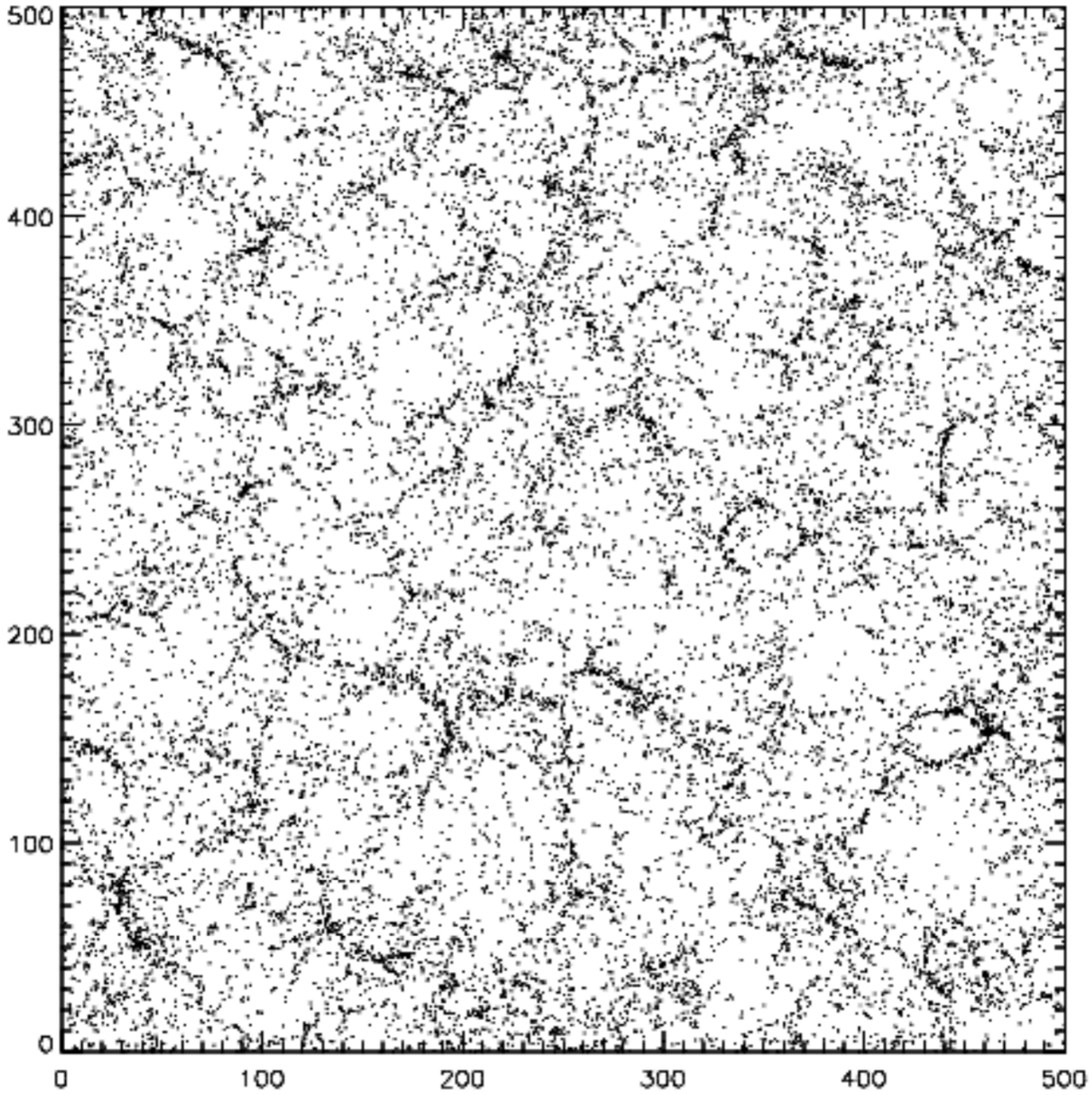

Gao, Springel & White 2005

The 20% of halos with the *earliest* half-mass assembly redshifts in a 30 Mpc/h thick slice

$$M_{halo} \sim 10^{11} M_{\odot}$$

Galaxy Clustering: Assembly bias - III

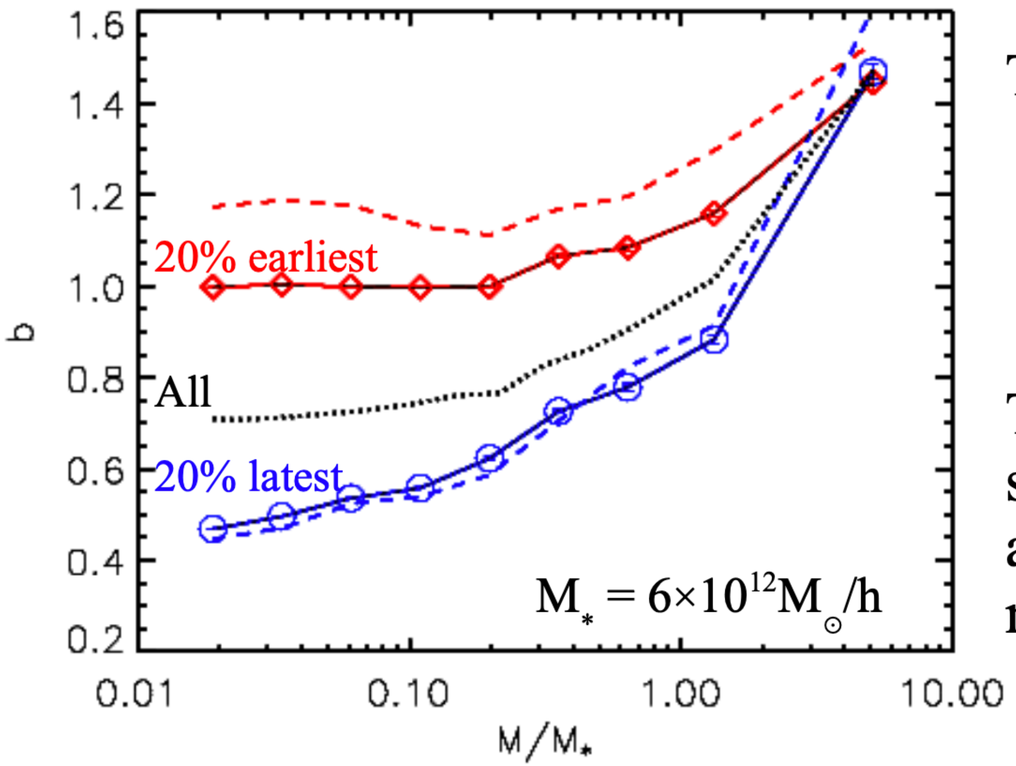

The dependence of bias on formation redshift is strongest at low mass

This behaviour is inconsistent with simple versions of excursion set theory, and of HOD and halo abundance matching models

Halo bias will not depend only on halo mass but also:

formation time
concentration
substructure content
spin
shape
saddle density
velocity anisotropy
.....

Problems for HOD
Halo Occupation Distribution
Approaches

including Intensity Mapping mocks-like approaches

Baryonic Acoustic Oscillations

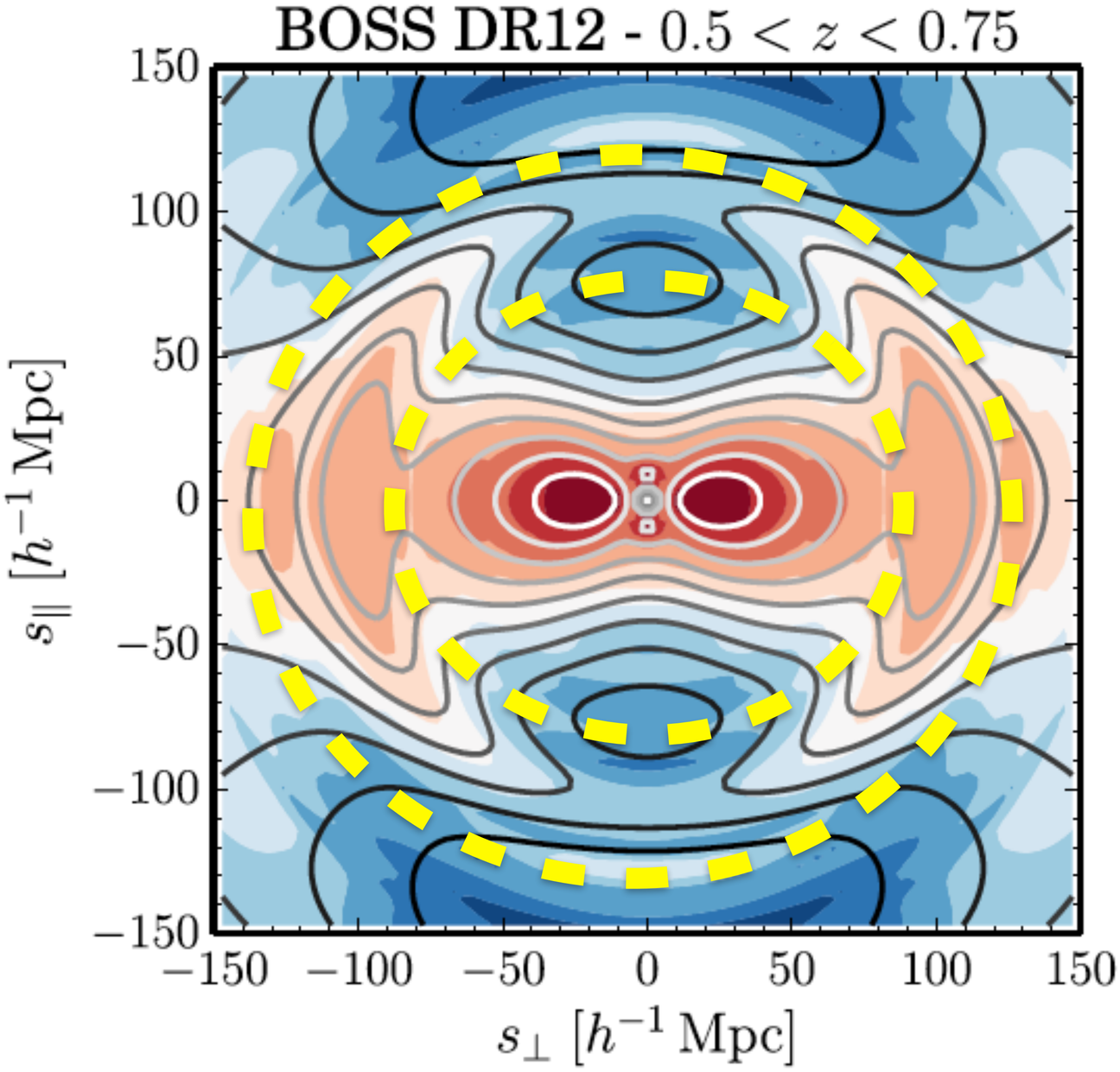

Combined effect of:

1) BAO
2) RSDs
3) for theory modelling (Alcock-Paczynski test)

The acoustic wave

Start with a single perturbation. The plasma is totally uniform except for an excess of matter at the origin.
High pressure drives the gas+photon fluid outward at speeds approaching the speed of light.

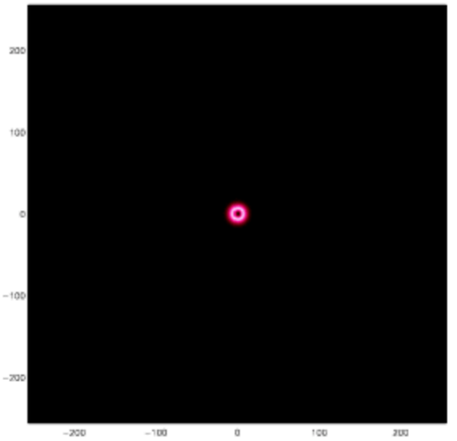

Baryons

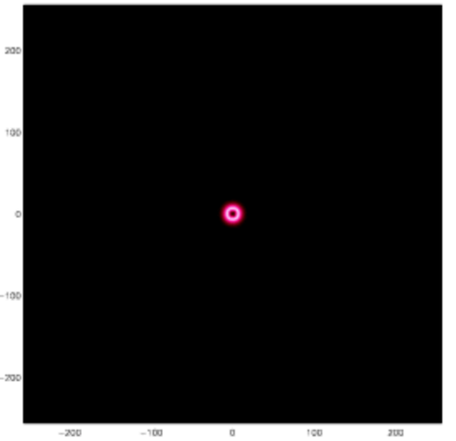

Photons

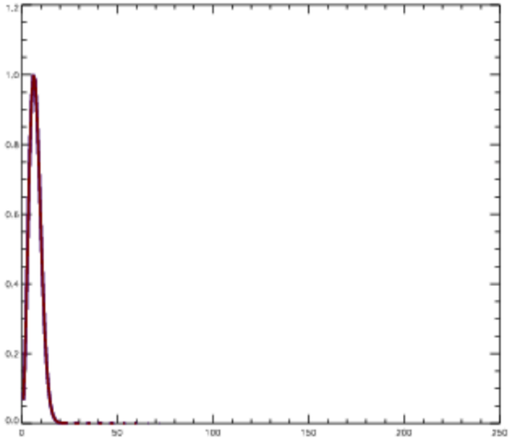

Mass profile

Eisenstein, Seo & White (2006)

The acoustic wave

Initially both the photons and the baryons move outward together, the radius of the shell moving at over half the speed of light.

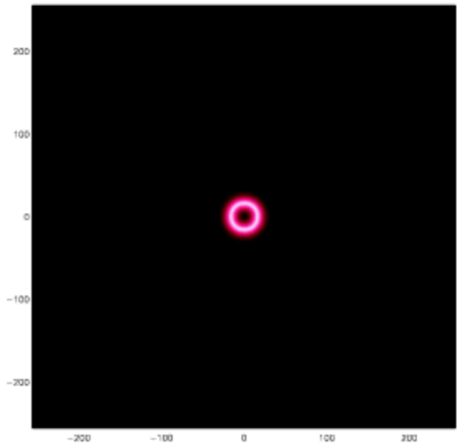

Baryons

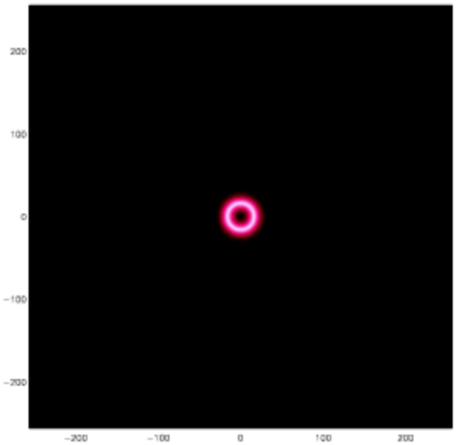

Photons

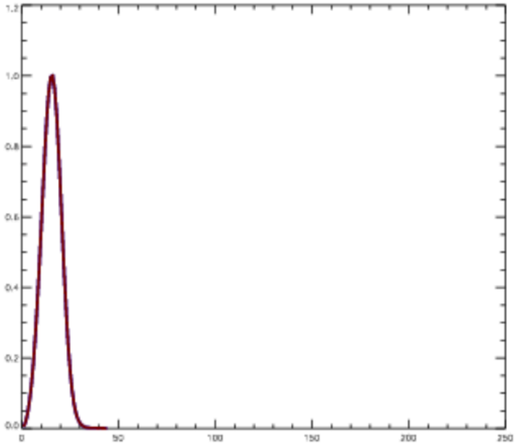

The acoustic wave

This expansion continues for 10^5 years

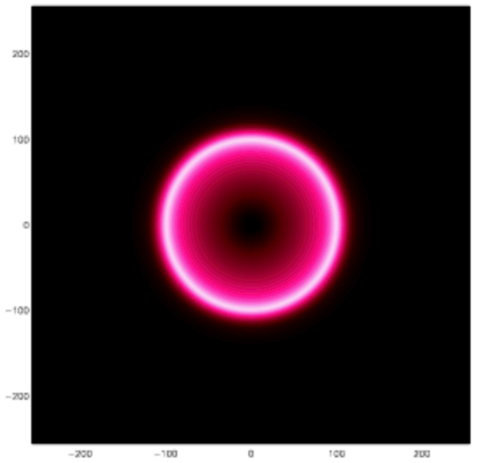

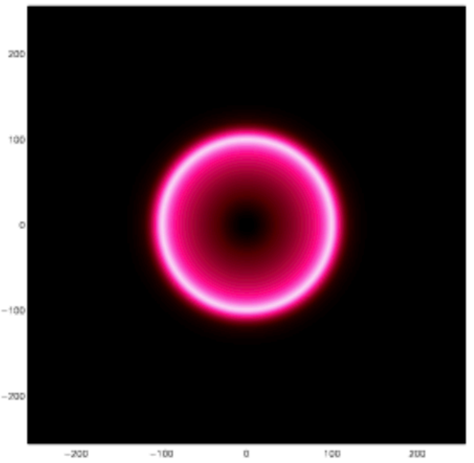

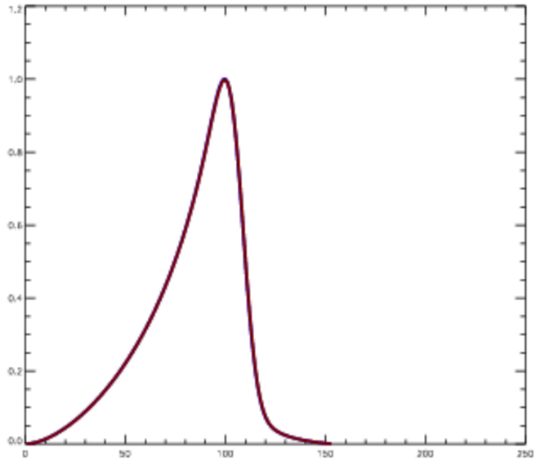

The acoustic wave

After 10^5 years the universe has cooled enough the protons capture the electrons to form neutral Hydrogen. This decouples the photons from the baryons. The former quickly stream away, leaving the baryon peak stalled.

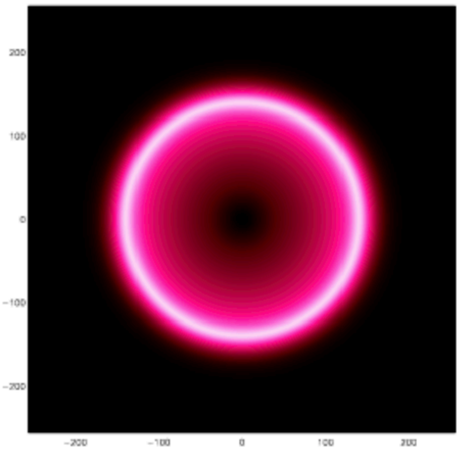

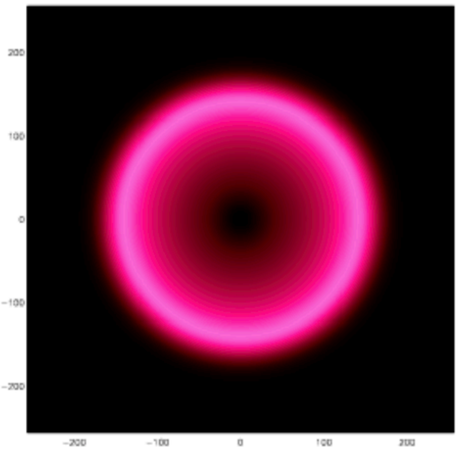

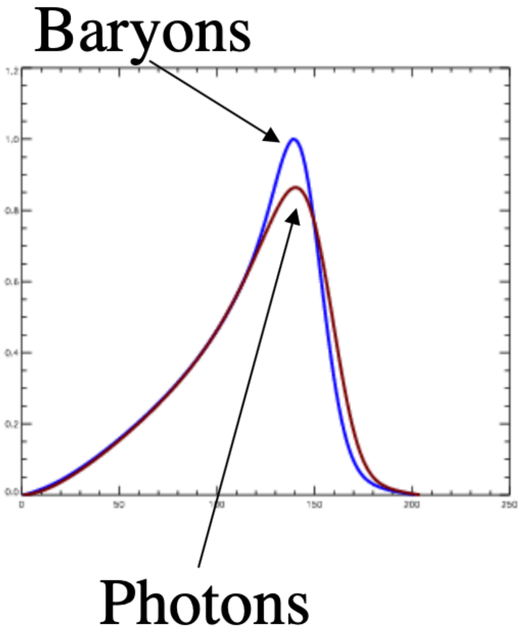

The acoustic wave

The photons continue to stream away while the baryons, having lost their motive pressure, remain in place.

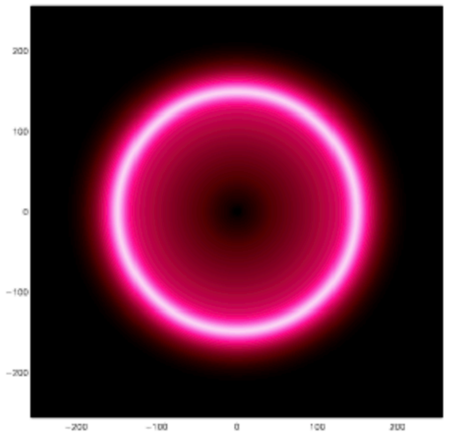

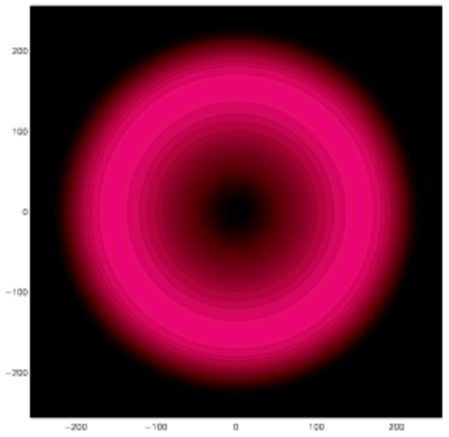

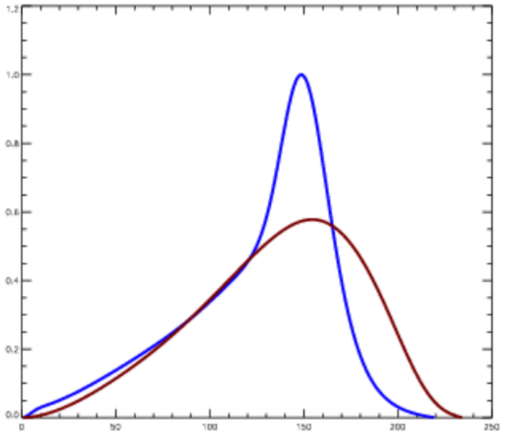

The acoustic wave

The photons have become almost completely uniform, but the baryons remain overdense in a shell 100Mpc in radius.
In addition, the large gravitational potential well which we started with starts to draw material back into it.

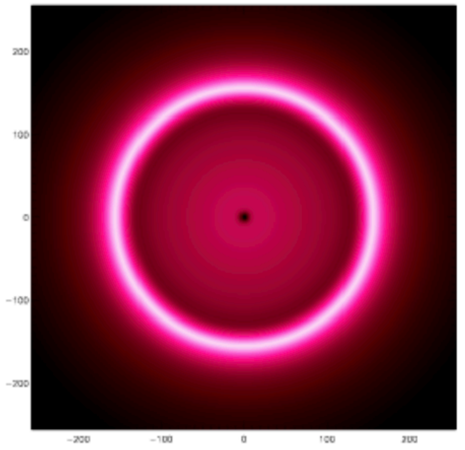

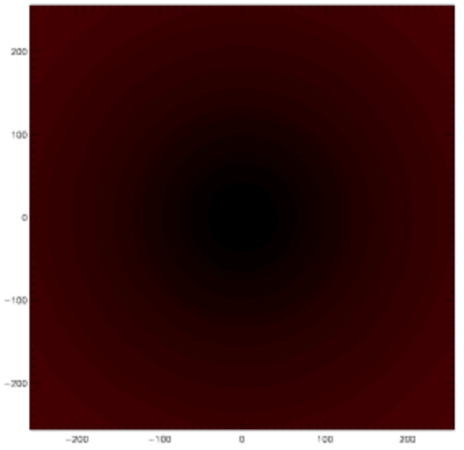

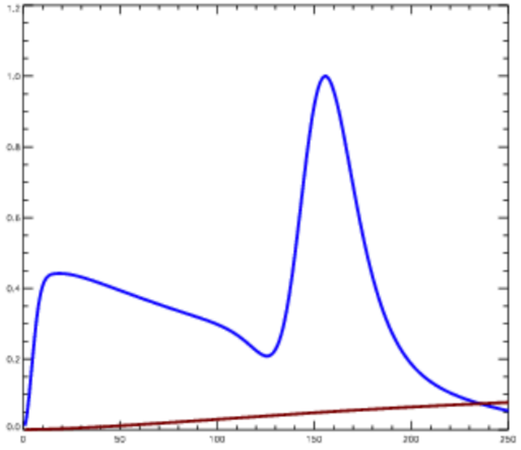

The acoustic wave

As the perturbation grows by ~10^3 the baryons and DM reach equilibrium densities in the ratio Ω_b/Ω_m.

The final configuration is our original peak at the center (which we put in by hand) and an "echo" in a shell roughly 100Mpc in radius.

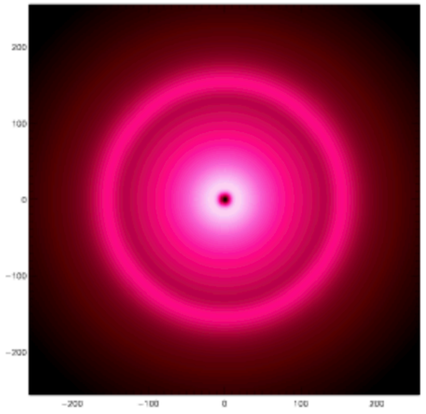

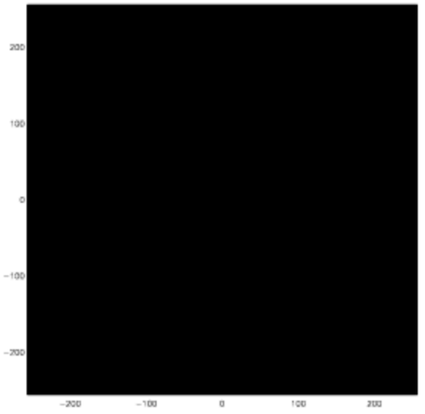

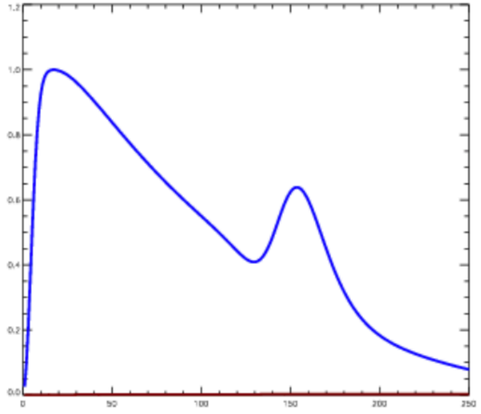

Further (non-linear) processing of the density field acts to broaden and very slightly shift the peak -- but galaxy formation is a local phenomenon with a length scale ~10Mpc, so the action at r=0 and r~100Mpc are essentially decoupled. We will return to this …

Galaxy Clustering - I: Theoretical Framework

Analysis of **anisotropic correlation function** focussed on the BAO signal

Two sources of anisotropies: Redshift Space Distortion (RSD)
Geometrical induced anisotropy (AP)

$$\xi(r,\mu) = \frac{\mathrm{DD}(r,\mu) - 2\mathrm{DR}(r,\mu) + \mathrm{RR}(r,\mu)}{\mathrm{RR}(r,\mu)}, \qquad \xi_\ell(r) = \frac{2\ell+1}{2}\int_{-1}^{+1} \mathrm{d}\mu\, \xi(r,\mu)\, L_\ell(\mu)$$

Non-linear modelling of correlation function

$$P(k,\mu) = (1+\beta\mu^2)^2 F(k,\mu,\Sigma_\mathrm{s}) P_\mathrm{NL}(k,\mu).$$

$$F(k,\mu,\Sigma_\mathrm{s}) = \frac{1}{(1+k^2\mu^2\Sigma_\mathrm{s}^2)}$$

$$P_\mathrm{dw}(k,\mu) = [P_\mathrm{lin}(k) - P_\mathrm{nw}(k)] \times \exp\left[-\frac{k^2\mu^2\Sigma_{||}^2 + k^2(1-\mu^2)\Sigma_\perp^2}{2}\right] + P_\mathrm{nw}$$

$$P_{\mathrm{l,t}}(k) = \frac{2l+1}{2}\int_{-1}^{1} P_t(k,\mu) L_\mathrm{l}(\mu)\mathrm{d}\mu$$

$$\xi_0(r) = B_0^2\xi_{0,\mathrm{t}}(r) + A_0(r),$$
$$\xi_2(r) \quad = \xi_{2,\mathrm{t}}(r) + A_2(r),$$

where

$$\xi_{\mathrm{l,t}}(r) = i^l \int \frac{k^3\,\mathrm{d}\log(k)}{2\pi^2} P_{\mathrm{l,t}} j_\mathrm{l}(kr),$$

$$A_\ell(r) = \frac{a_{\ell,1}}{r^2} + \frac{a_{\ell,2}}{r} + a_{\ell,3};\ \ell = 0, 2, \perp, \|$$

Galaxy Clustering - II: Theoretical Framework

$$\alpha = \alpha_{\perp}^{2/3}\alpha_{||}^{1/3},$$

$$1+\epsilon = \left(\frac{\alpha_{||}}{\alpha_{\perp}}\right)^{1/3}$$

$$\alpha_{\perp} = \frac{D_{\rm A}(z)r_{\rm s}^{\rm fid}}{D_{\rm A}^{\rm fid}r_{\rm s}}$$

$$\alpha_{||} = \frac{H^{\rm fid}(z)r_{\rm s}^{\rm fid}}{H(z)r_{\rm s}}$$

α, ε usually appear when referring to systematics/mocks while distances and F_{AP} when quoting final cosmologically relevant numbers

$$D_V(z) = \left(D_M^2(z)\frac{cz}{H(z)}\right)^{1/3}$$

$$F_{\rm AP}(z) = D_M(z)H(z)/c.$$

Galaxy clustering challenges - ca 2020

Measurement of galaxy clustering hampered by **systematics** and **statistical** errors.

Estimating the window function and selection function is not trivial.

Focus on:

1) optimization of codes to handle large number of objects
2) getting reliable mocks
3) quantifying systematic effects
4) covariance matrix estimation
5) improving **reconstruction techniques**

State-of-the-art provided by BOSS survey (e.g. Alam+18, Vargas-Magana+18)

1) Systematics are estimated and appear as weights in the selection function
2) Mock generation using several different methods - based on Perturbation theory or N-body simulations
3) Estimation of the 2D correlation function using Landy-Szalay estimator
4) Analysis focused on BAO peak and in second instance on sub-BAO **shape** info
5) Different pipelines tested with estimation of systematic errors introduced in each step
6) Main conclusions: unlike naively expected latest BOSS results **are dominated by statistical errors**

Galaxy clustering: the data set

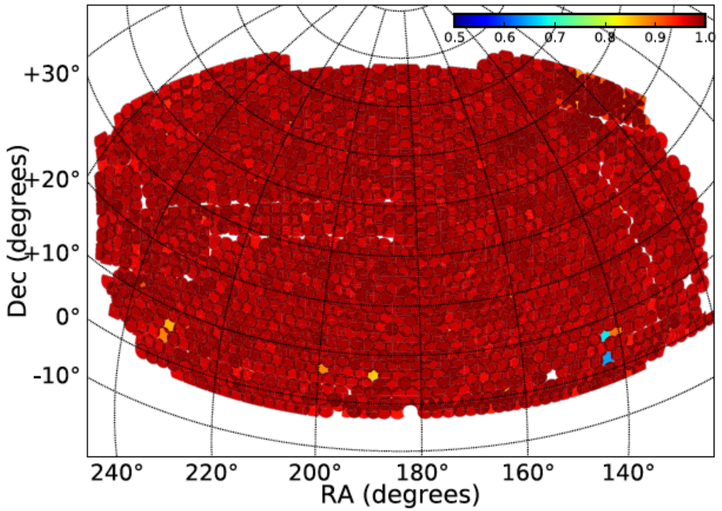

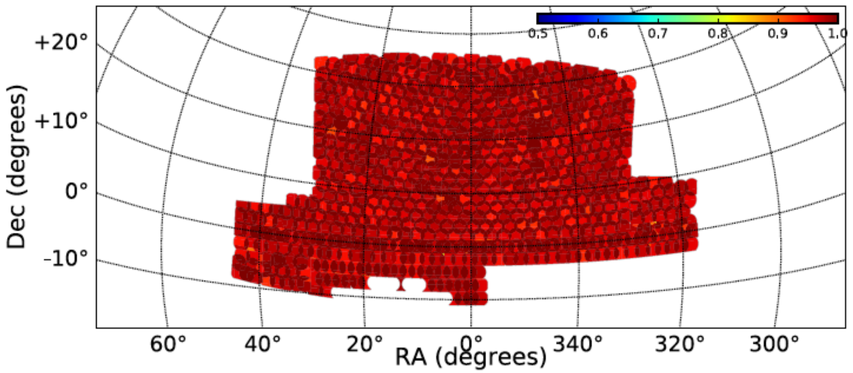

10,000 sq. deg. & 1.2 million galaxies in V=20 Gpc^3

medium-resolution spectra (R ≈ 1500–2600) in the wavelength range from 3600 to 10000 Å through 2 arcsec fibres

LOWZ was designed to target luminous red galaxies up to z ≈ 0.4, while CMASS was designed to target massive galaxies from 0.4 < z < 0.7

Seven data analyses performed with different methodologies (tested on mocks)

		N_{gals}	V_{eff} (Gpc^3)	V (Gpc^3)
$0.2 < z < 0.5$	NGC	429 182	2.7	4.7
	SGC	174 819	1.0	1.7
	Total	604 001	3.7	6.4
$0.4 < z < 0.6$	NGC	500 872	3.1	5.3
	SGC	185498	1.1	2.0
	Total	686 370	4.2	7.3
$0.5 < z < 0.75$	NGC	435 741	3.0	9.0
	SGC	158 262	1.1	3.3
	Total	594 003	4.1	12.3

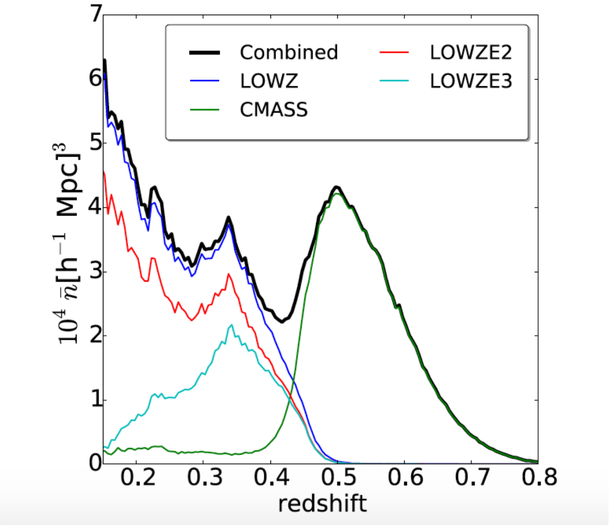

Galaxy clustering: the signal

Analysis performed in configuration and Fourier space and gives consistent results

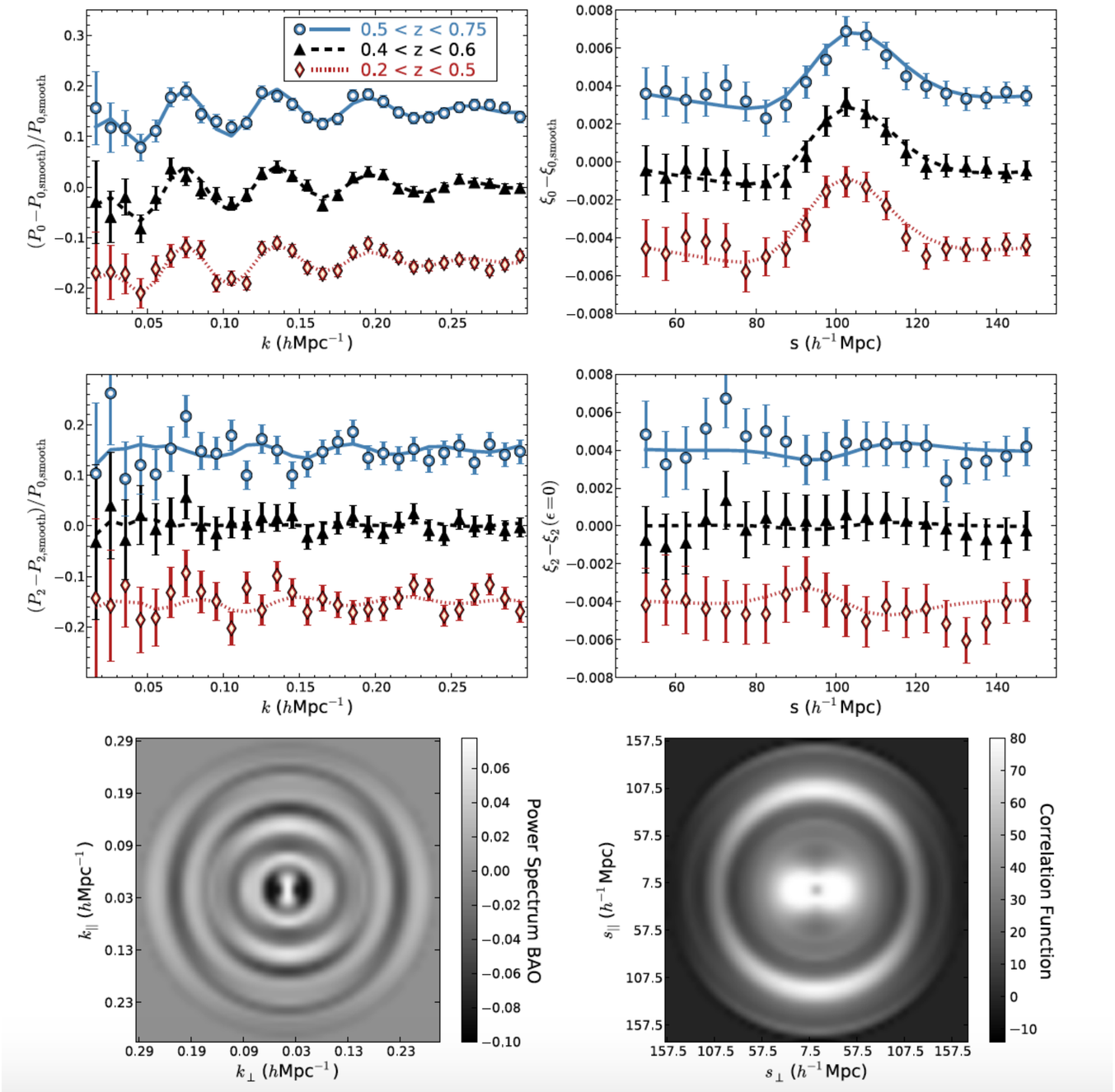

Galaxy clustering: constraints from BAOs

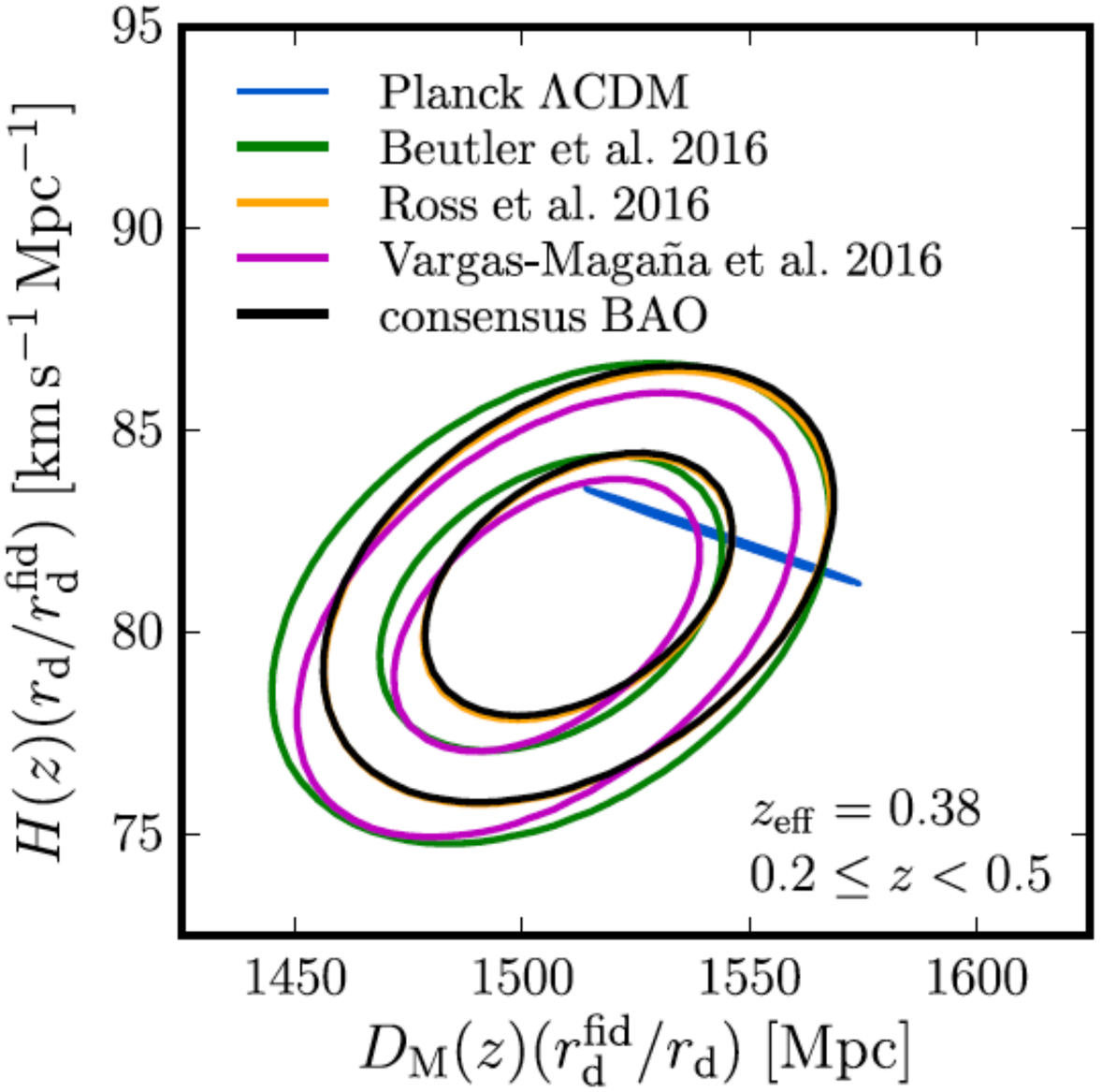

BAO measurement combined with CMB prior allows to measure H(z) at 2.4% and $D_A(z)$ at 1.5% in each redshift bin When combined $D_A(z)$ measured at 1% and H(z) at 1.6%

Perfect agreement with Planck

remarkable measurements not su much freedom to escape from LCDM

Consensus costraints are obtained by combined up to 7 different methods with strong covariance (mock estimated) but they improve the overall constraint significantly.

Galaxy clustering: constraints from full shape

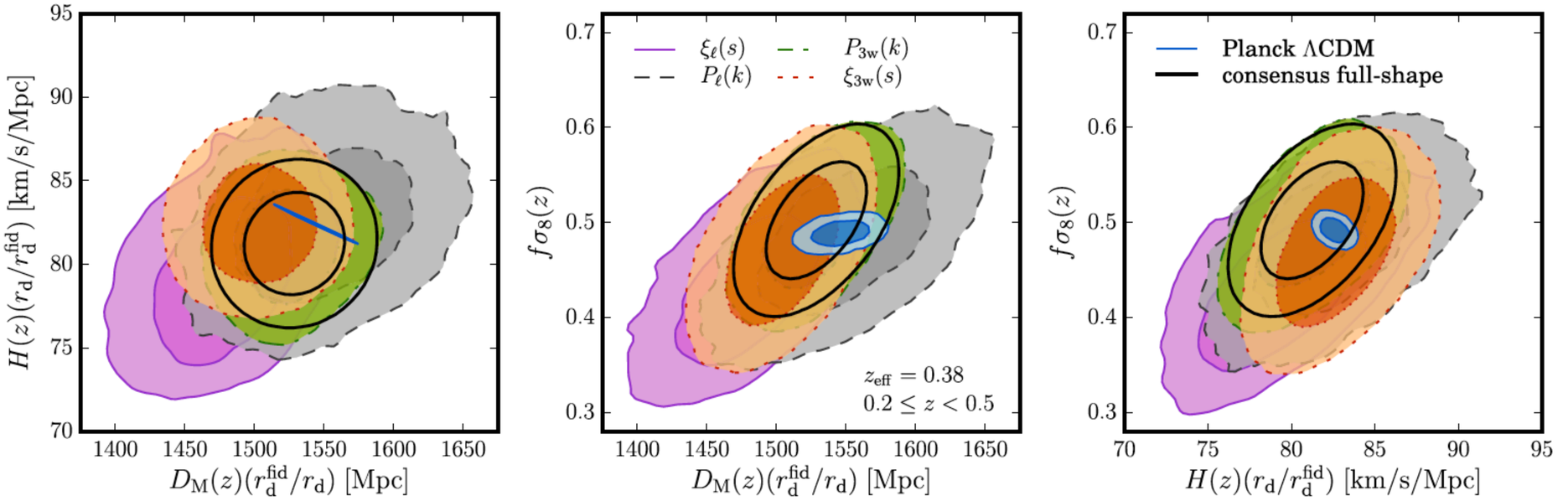

Full-shape measurement with a variety of methods, this allows to measure the $f\sigma_8$ combination with a 10% precision in each bin and overall a 6% measurement

Perfect agreement with Planck

BAO+full shape combined

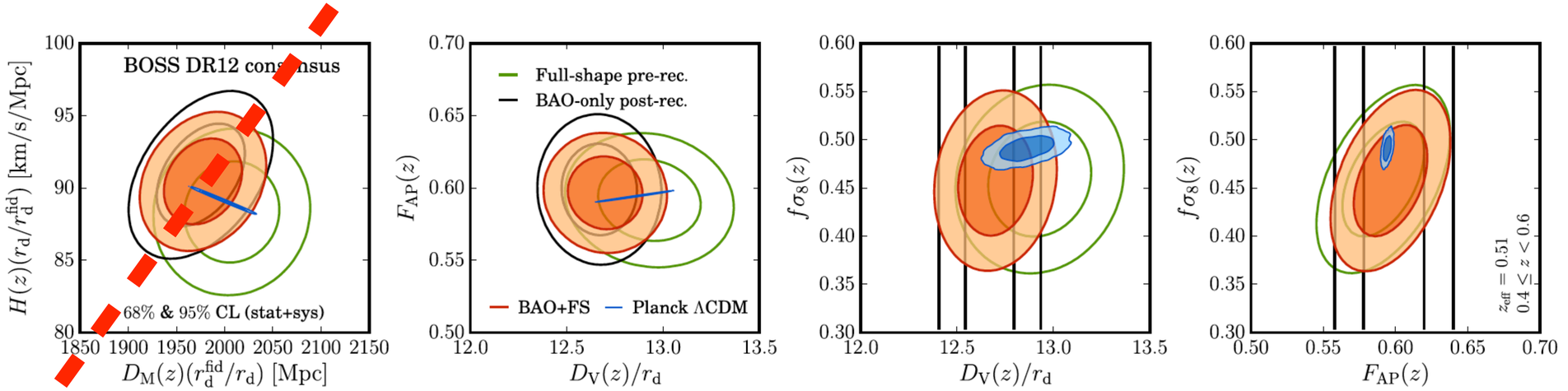

$D_M(z)$ and $H(z)$ are more strongly correlated for the BAO-only analysis, so while the $D_V(z)$ constraints from postreconstruction BAO-only are appreciably tighter than those from pre-reconstruction FS, the marginalized constraints on DM(z) and H(z) are not.

The constraints on $F_{AP}(z)$ from sub-BAO scales in the FS analyses help to **break the degeneracy** between D_M and H, leading to rounder confidence contours and smaller errors on FAP.

Combined BAO+FS contours take advantage of both the **sharpening** of the BAO feature by reconstruction and the improved **degeneracy breaking from the sub-BAO Alcock–Paczynski effect.**

Constraints from post-reconstruction BAO measurements and pre-reconstruction full-shape

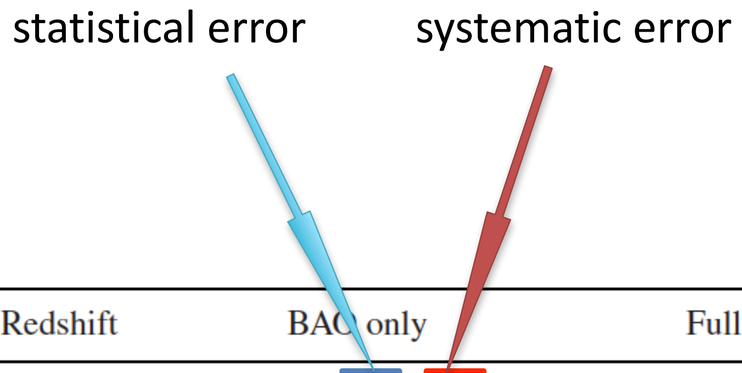

Measurement	Redshift	BAO only	Full shape	BAO + FS
$D_M(r_{\rm d,\,fid}/r_{\rm d})$ (Mpc)	$z = 0.38$	$1512 \pm 22 \pm 11$	$1529 \pm 24 \pm 11$	$1518 \pm 20 \pm 11$
$D_M(r_{\rm d,\,fid}/r_{\rm d})$ (Mpc)	$z = 0.51$	$1975 \pm 27 \pm 14$	$2007 \pm 29 \pm 15$	$1977 \pm 23 \pm 14$
$D_M(r_{\rm d,\,fid}/r_{\rm d})$ (Mpc)	$z = 0.61$	$2307 \pm 33 \pm 17$	$2274 \pm 36 \pm 17$	$2283 \pm 28 \pm 16$
$H(r_{\rm d}/r_{\rm d,\,fid})$ (km s^{-1}Mpc^{-1})	$z = 0.38$	$81.2 \pm 2.2 \pm 1.0$	$81.2 \pm 2.0 \pm 1.0$	$81.5 \pm 1.7 \pm 0.9$
$H(r_{\rm d}/r_{\rm d,\,fid})$ (km s^{-1}Mpc^{-1})	$z = 0.51$	$90.9 \pm 2.1 \pm 1.1$	$88.3 \pm 2.1 \pm 1.0$	$90.5 \pm 1.7 \pm 1.0$
$H(r_{\rm d}/r_{\rm d,\,fid})$ (km s^{-1}Mpc^{-1})	$z = 0.61$	$99.0 \pm 2.2 \pm 1.2$	$95.6 \pm 2.4 \pm 1.1$	$97.3 \pm 1.8 \pm 1.1$
$f\sigma_8$	$z = 0.38$	–	$0.502 \pm 0.041 \pm 0.024$	$0.497 \pm 0.039 \pm 0.024$
$f\sigma_8$	$z = 0.51$	–	$0.459 \pm 0.037 \pm 0.015$	$0.458 \pm 0.035 \pm 0.015$
$f\sigma_8$	$z = 0.61$	–	$0.419 \pm 0.036 \pm 0.009$	$0.436 \pm 0.034 \pm 0.009$

BAO Hubble Diagram and Growth

Alam+20

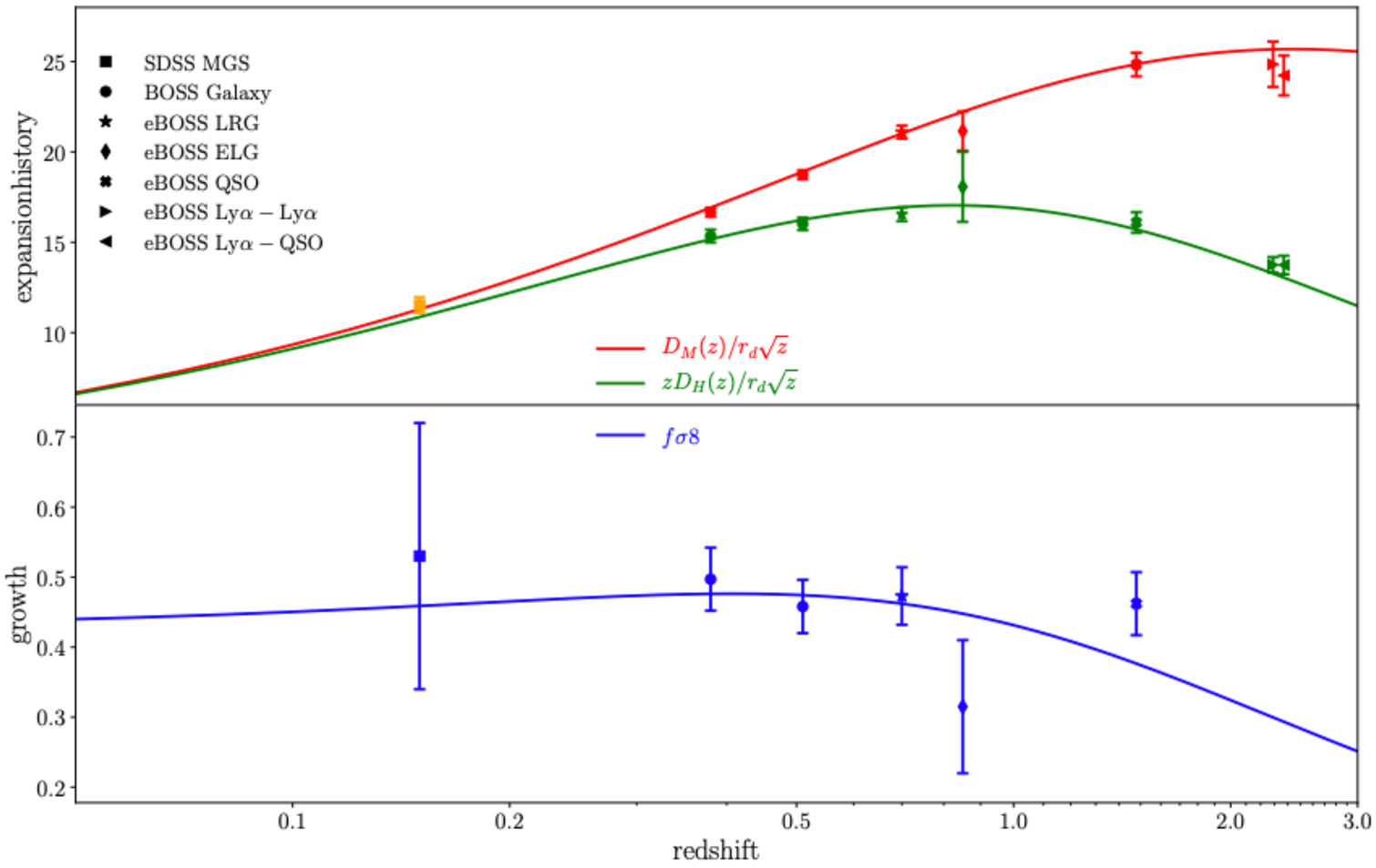

BAO constraints at high and low redshift

CMASS BAO

Aubourg+15

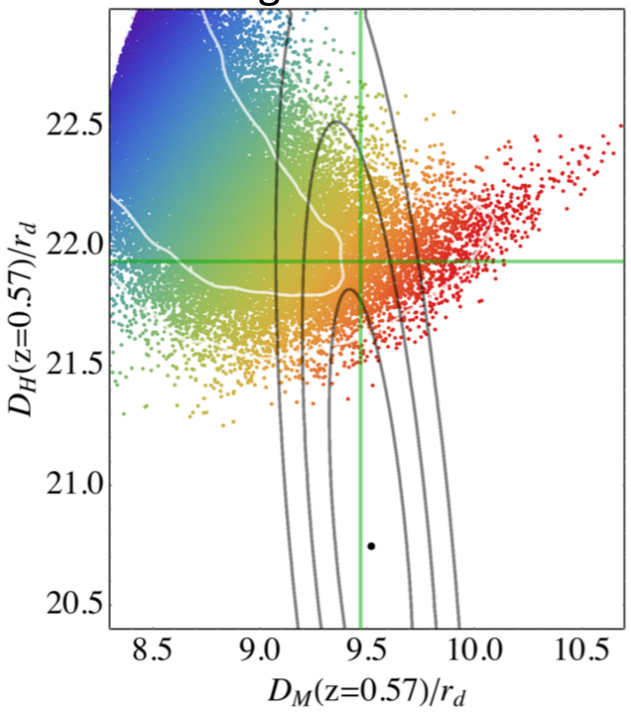

Lyalpha BAO

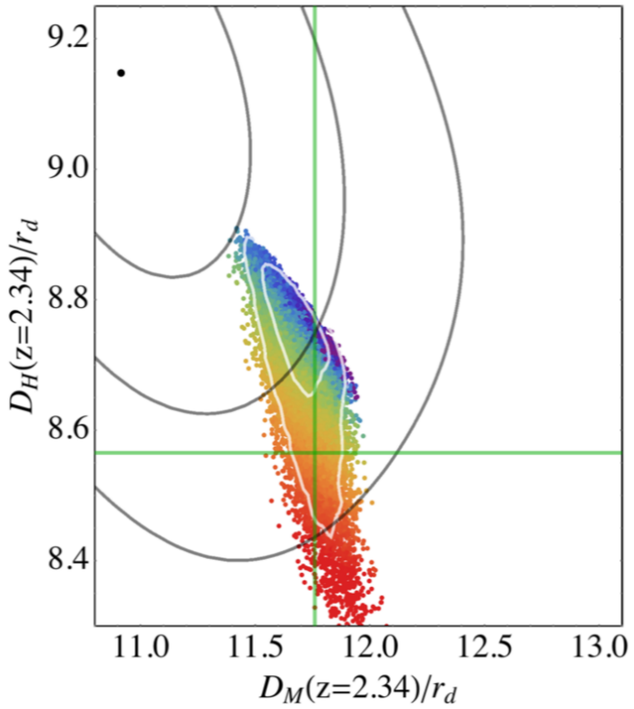

Planck wCDM

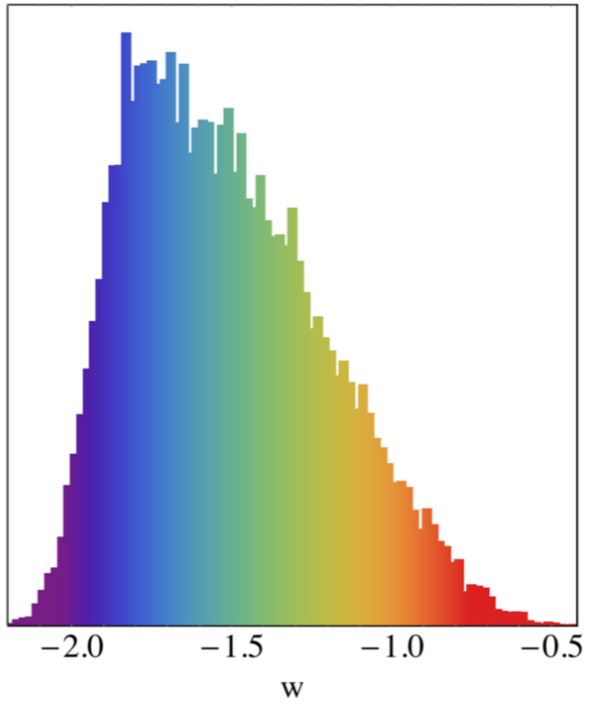

Tensions between Lya BAO and CMASS BAO

In general Early DE models can alleviate tensions of LCDM (low clustering amplitude and large H_0 are predicted at low z)

RSD measurements from BOSS

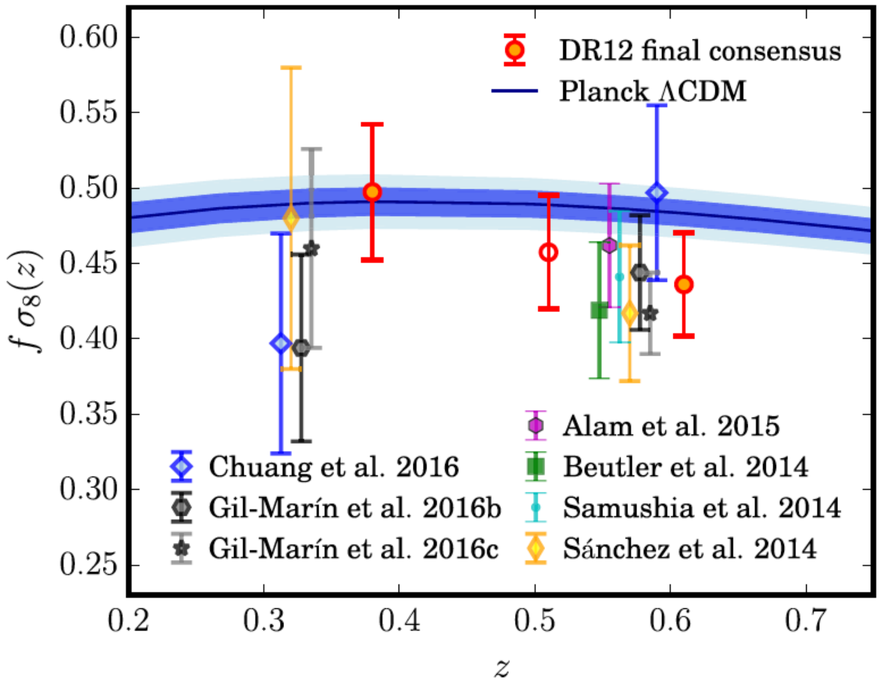

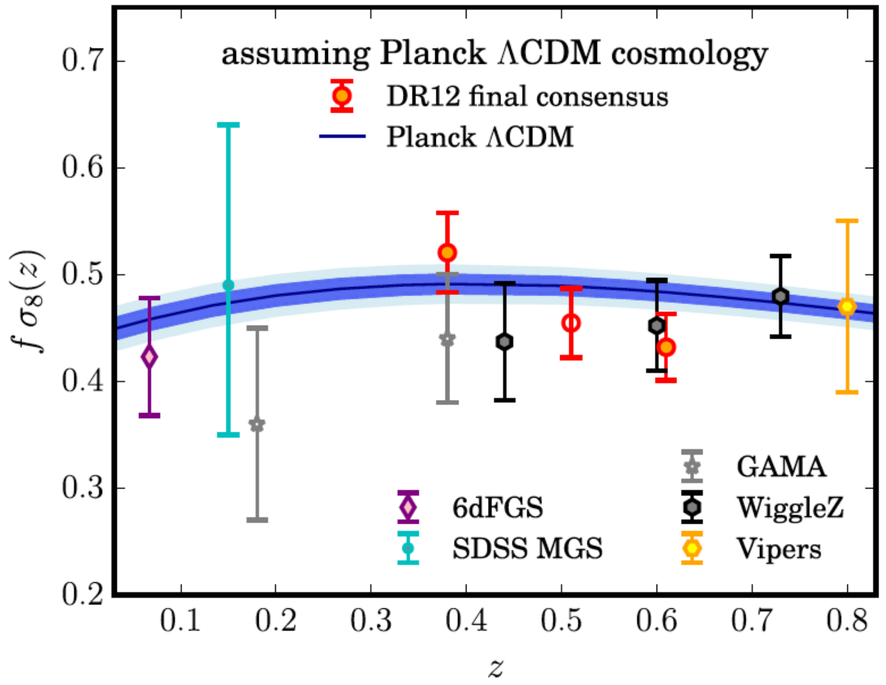

Planck + BOSS galaxy clustering - I

In the LCDM case Ω_m=0.311 ± 0.006 and H_0=67.6 ± 0.5 km/s/Mpc

If Ω_k and w are varied Ω_k=0.0003 ± 0.0026 and w=-1.01 ± 0.06

owCDM model

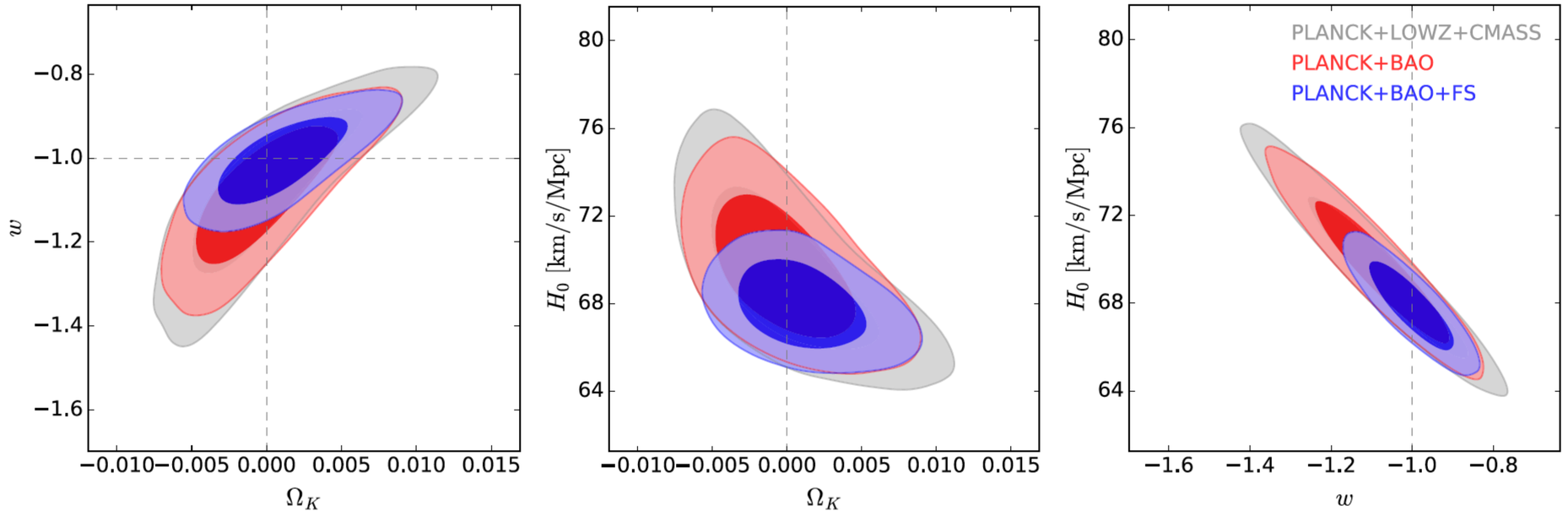

Main results:

1) impressive agreement with LCDM even after opening a 2 parameter space (w, Ω_k)
2) FOM for wCDM ~20-30
3) Adding z-bins helps

Planck + BOSS galaxy clustering - II

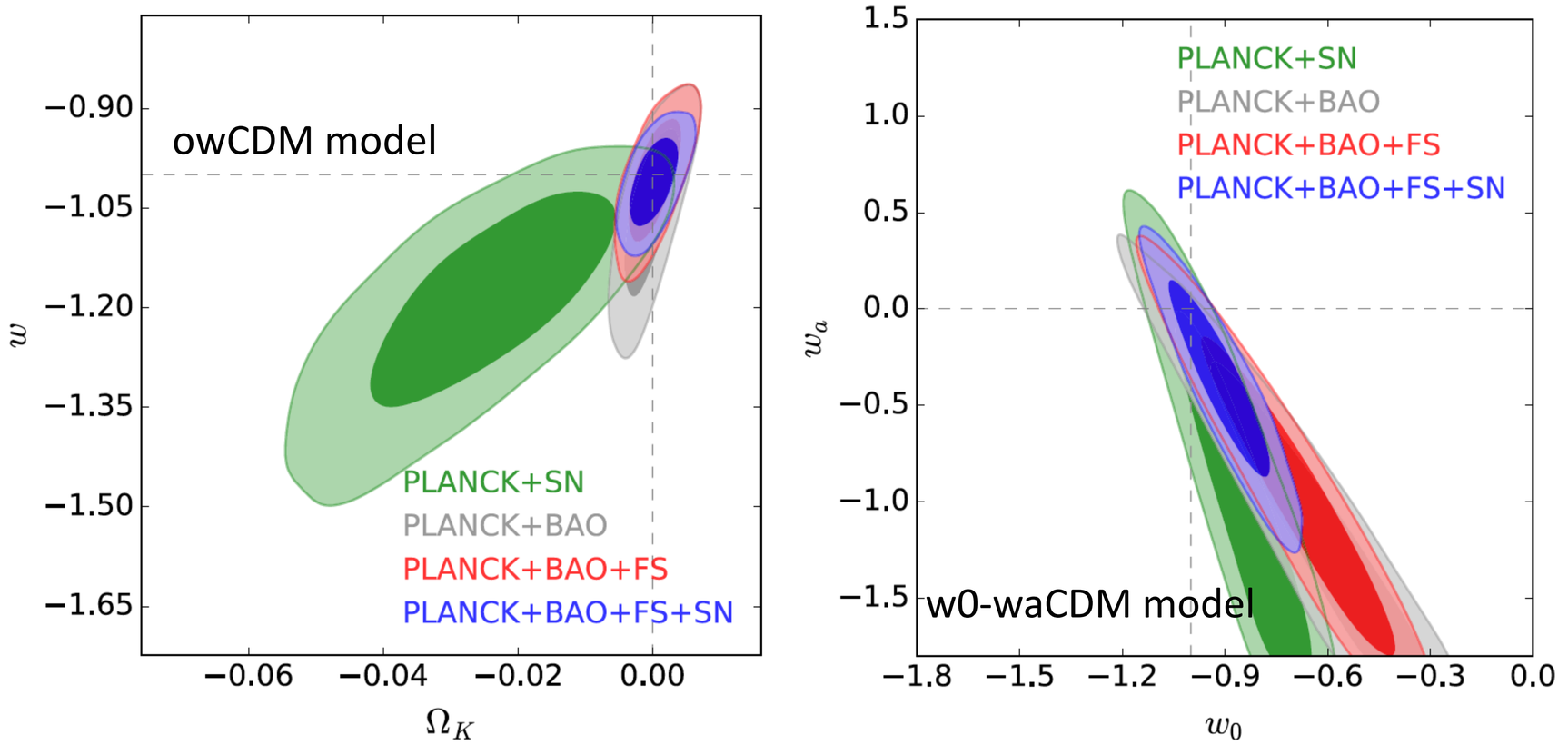

Cosmological model	Data sets	$\Omega_m h^2$	Ω_m	H_0 (km s^{-1} Mpc^{-1})	Ω_K	w_0	w_a
w_0w_aCDM	Planck + SN	0.1428 (14)	0.294 (16)	69.8 (18)	–	−0.85 (13)	−0.99 (63)
w_0w_aCDM	Planck + BAO	0.1427 (11)	0.336 (21)	65.2 (21)	–	−0.63 (20)	−1.16 (55)
w_0w_aCDM	Planck + BAO + FS	0.1427 (11)	0.334 (18)	65.5 (17)	–	−0.68 (18)	−0.98 (53)
w_0w_aCDM	Planck + BAO + FS + SN	0.1426 (11)	0.313 (9)	67.5 (10)	–	−0.91 (10)	−0.39 (34)
ow_0w_aCDM	Planck + BAO	0.1422 (14)	0.331 (21)	65.6 (21)	−0.0022 (30)	−0.66 (19)	−1.22 (53)
ow_0w_aCDM	Planck + BAO + FS	0.1422 (14)	0.333 (16)	65.4 (16)	−0.0020 (28)	−0.67 (18)	−1.12 (59)
ow_0w_aCDM	Planck + BAO + FS + SN	0.1420 (14)	0.314 (10)	67.3 (10)	−0.0023 (28)	−0.87 (11)	−0.63 (45)

Planck + BOSS galaxy clustering - III

$$f\sigma_8 \rightarrow f\sigma_8 \left[A_{f\sigma_8} + B_{f\sigma_8}(z - z_p)\right]$$

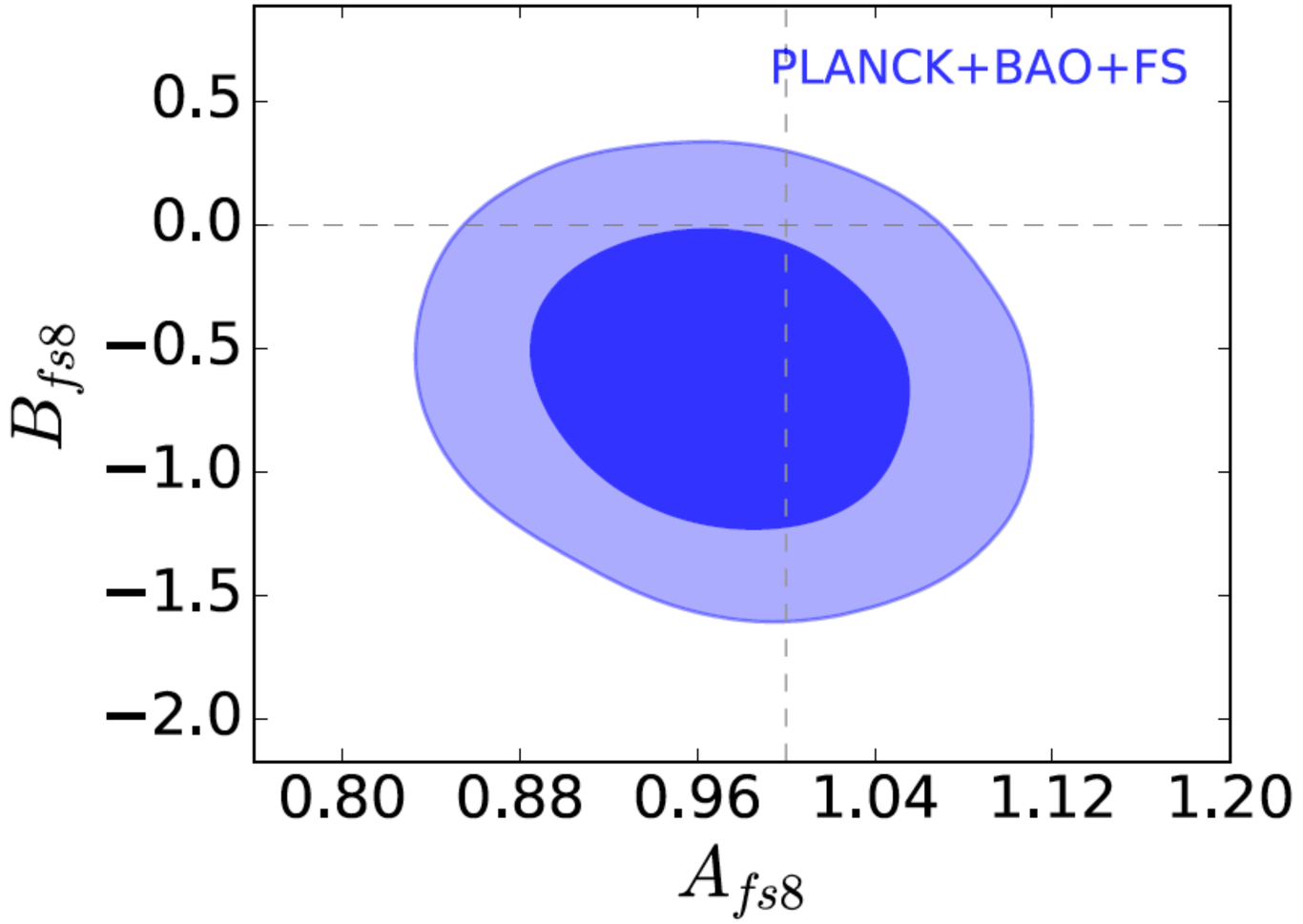

few percent offset from GR case - this is not significant

B is different from zero at 1.5sigma

6% error on A

Again very stable also when curvature and w are considered

How sensitive are we to sigma_8?

Envelope bracketing
s8=0.53-0.85

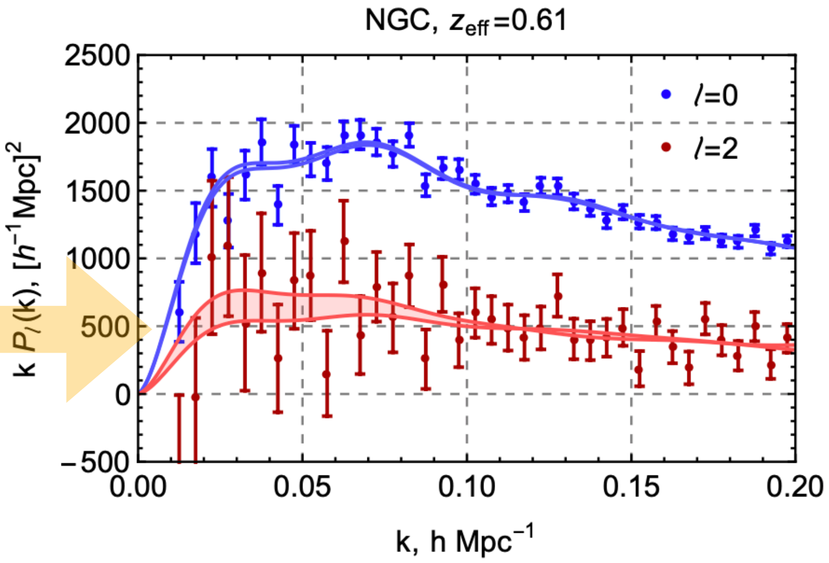

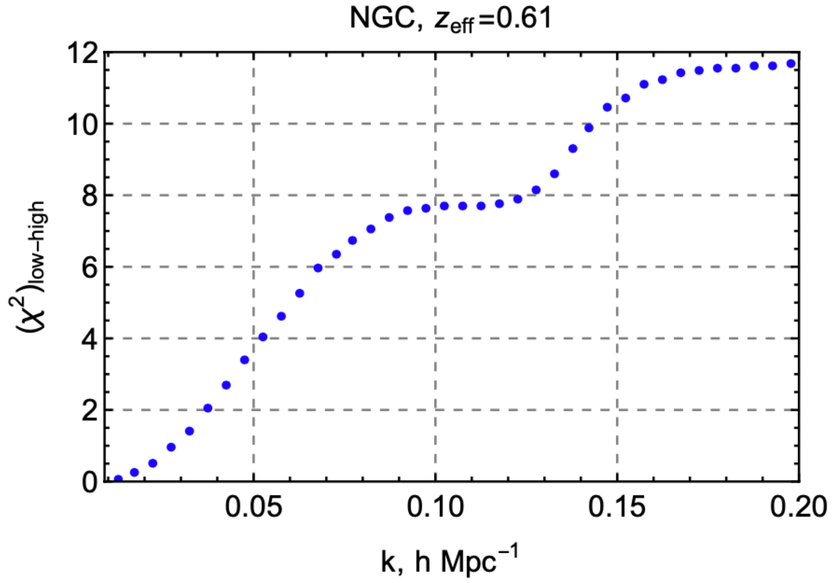

Philcox & Ivanov 22

Curvature

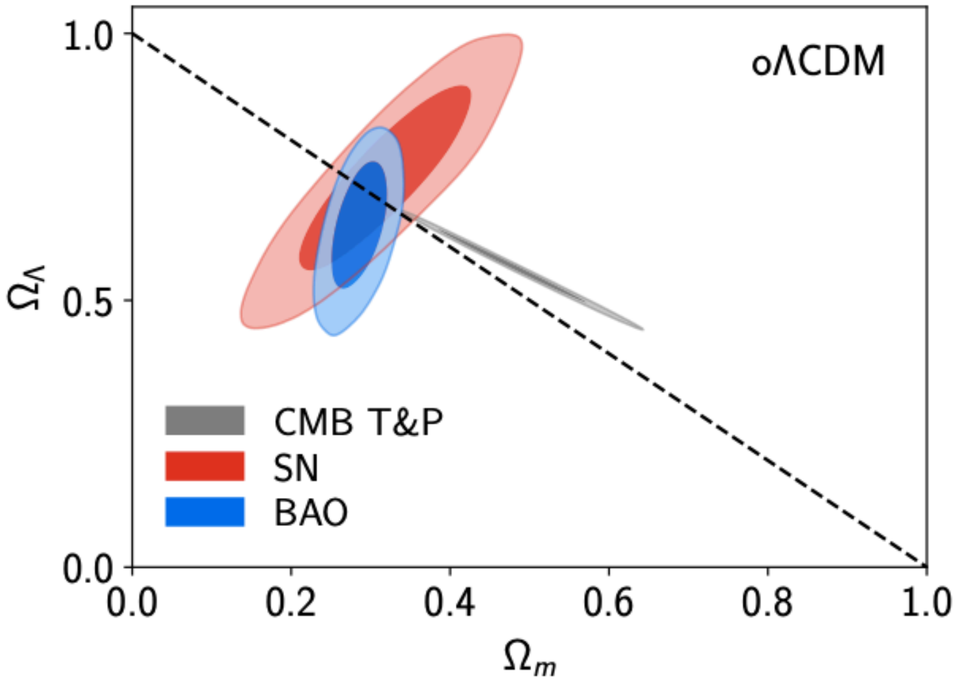
oΛCDM
1.0
0.5
0.0
Ω_Λ
0.0
0.2
0.4
0.6
0.8
1.0
Ω_m
CMB T&P
SN
BAO

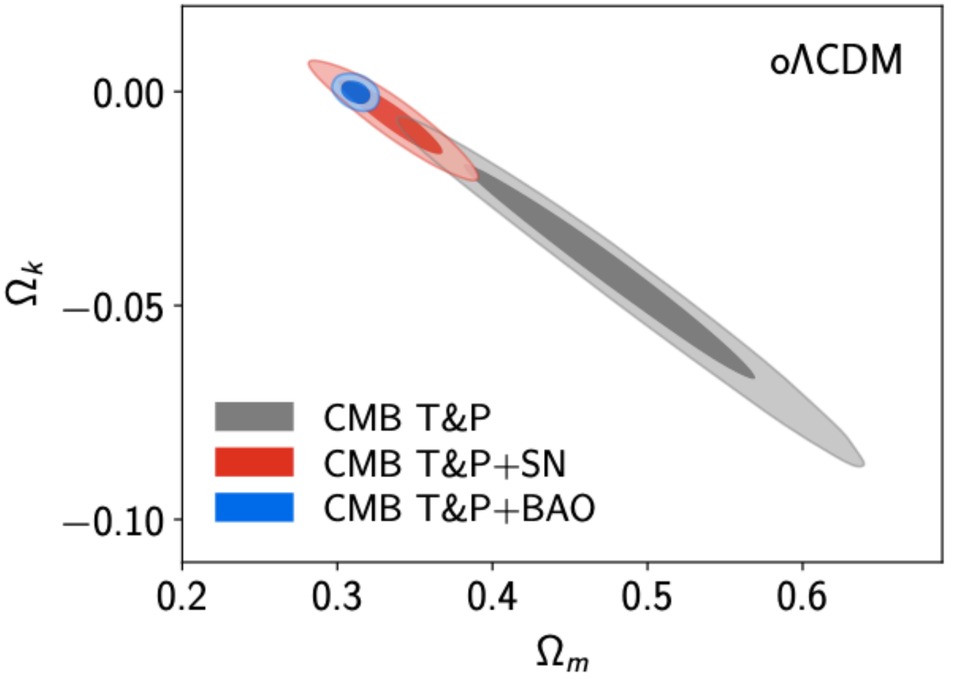
oΛCDM
0.00
−0.05
−0.10
Ω_k
0.2
0.3
0.4
0.5
0.6
Ω_m
CMB T&P
CMB T&P+SN
CMB T&P+BAO

Dark Energy OR neutrinos

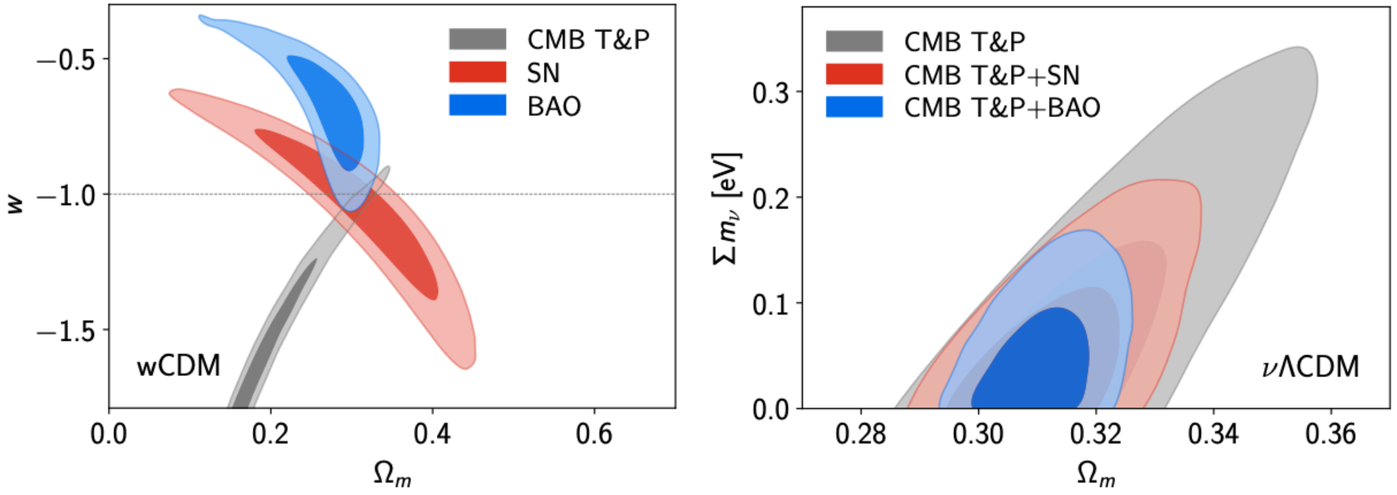

Dark Energy AND neutrinos

Semenaite+22

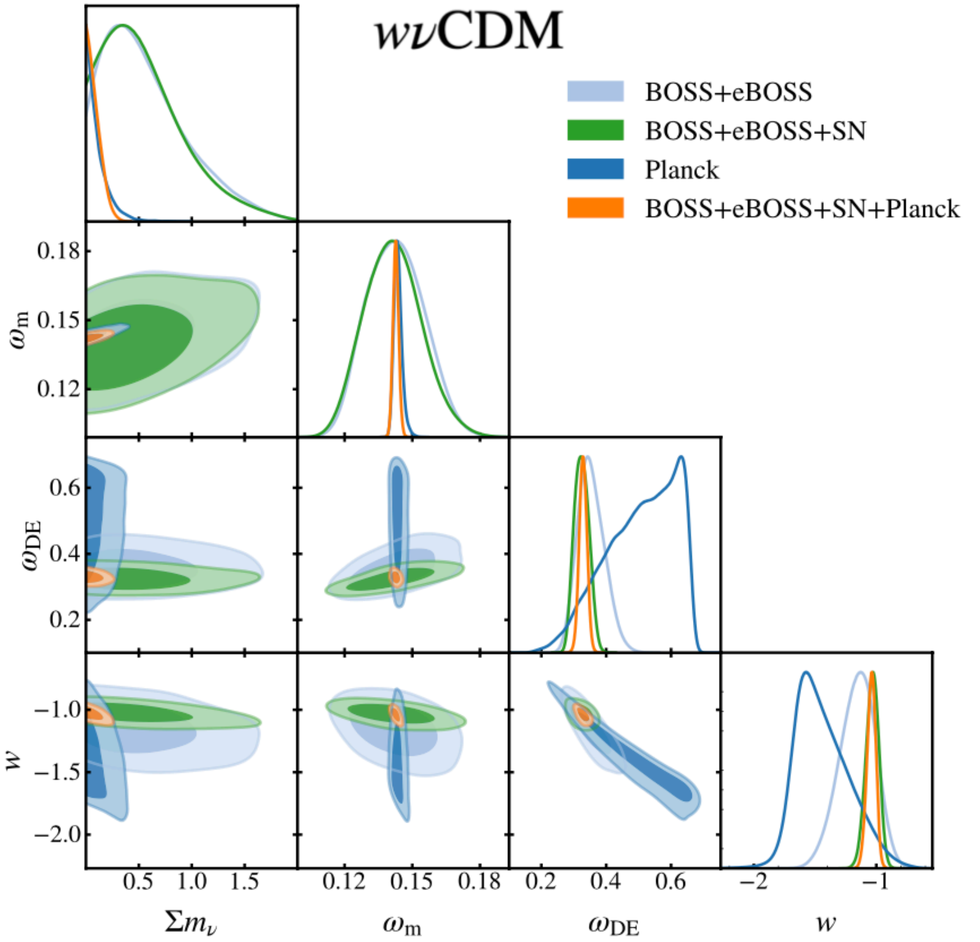

Mnu<0.211 eV (2sigma C.L.)

Matter Distribution at Small Scales

$$f\sigma_8 = \gamma_f \, f_{\Lambda\mathrm{CDM}}\sigma_8$$

v_{bc}: parameter that controls in the HOD how the central galaxy is distributed within the DM halo - non-linear velocity

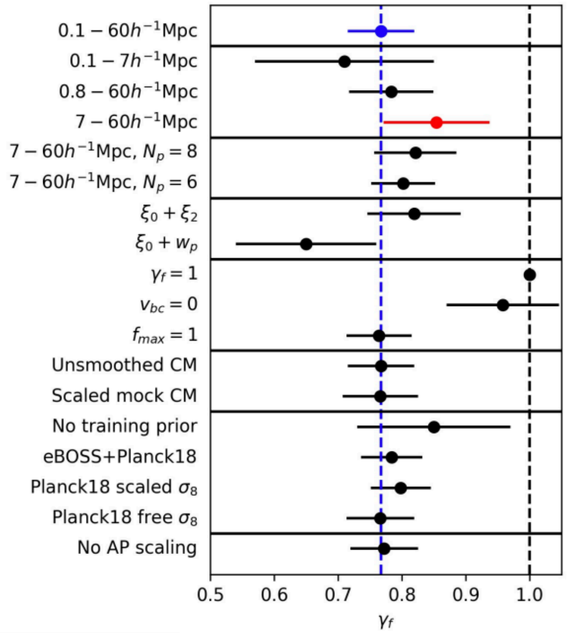

Chapman+21

- Consistent with ΛCDM on largest scales (1.4σ) matches "standard" RSD model that agree with ΛCDM expectation
- Deviations on small scales (up to 4.5σ) - RSD equivalent of "lensing is low" is "non-linear velocity dispersion is low"
  - Insufficient mass in halos?
  - HOD model break down?
  - Simulations wrong?
  - Systematic errors?

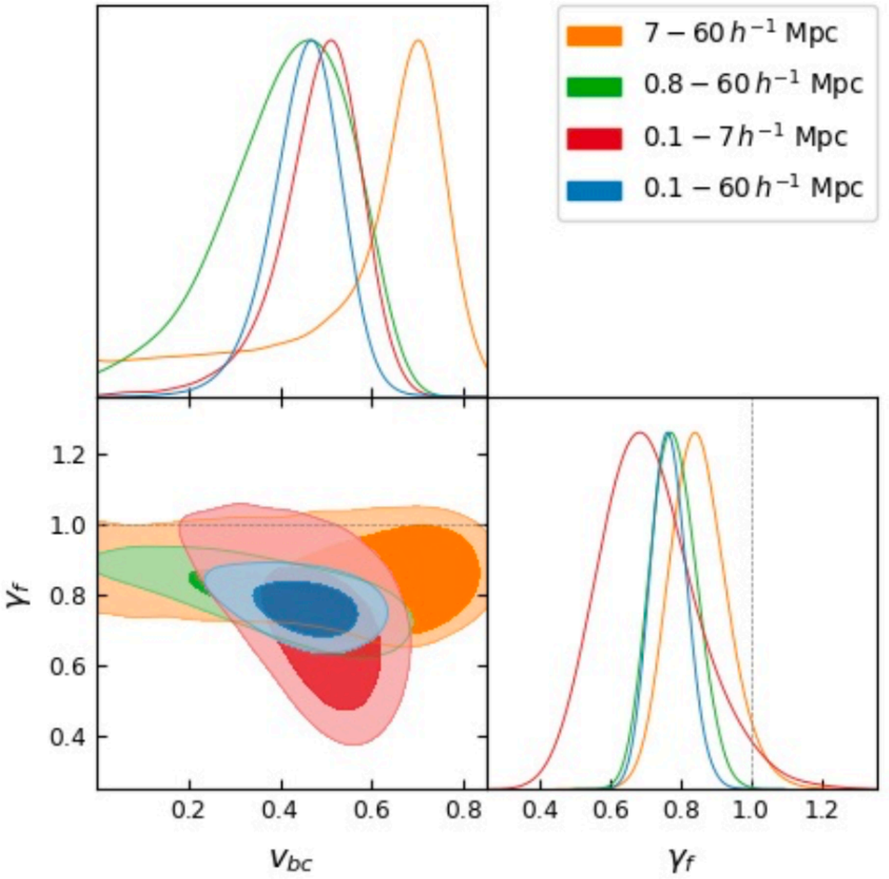

BOSS: main conclusions

1) ~1% constraints on H(z) and DA(z) from BAO

2) amplitude of pec. vel. measured at ~10% level

3) No evidence for physics beyond LCDM

4) Agreement with Planck low values for H0, with limits remarkably stable also for owCDM or ow0waCDM models with 1sigma error bar of 1km/s/Mpc

5) Limits on neutrino mass are 0.16 eV, which become 0.25 when removing RSD
and ~0.3 when opening the w parameter space

6) No support for Neff>3

OVERALL the stage is set and future seems promising for the next experiments like eBOSS, DESI, WFIRST/ROMAN, Euclid, LSST etc.
it is expected that statistical errors will improve and a new level of systematics will be hit (sub-percent precision constraints)

Latest analyses on galaxy clustering

The BOSS DR12 Full-Shape Cosmology:
ΛCDM Constraints from the Large-Scale Galaxy Power Spectrum and Bispectrum Monopol

Oliver H. E. Philcox[1,2,*] and Mikhail M. Ivanov[2,†]

[1] *Department of Astrophysical Sciences, Princeton University, Princeton, NJ 08540, USA*

[2] *School of Natural Sciences, Institute for Advanced Study, 1 Einstein Drive, Princeton, NJ 08540, USA*

We present a full ΛCDM analysis of the BOSS DR12 dataset, including information from the power spectrum multipoles, the real-space power spectrum, the reconstructed power spectrum and the bispectrum monopole. This is the first analysis to feature a complete treatment of the galaxy bispectrum, including a consistent theoretical model and without large-scale cuts. Unlike previous works, the statistics are measured using window-free estimators: this greatly reduces computational costs by removing the need to window-convolve the theory model. Our pipeline is tested using a suite of high-resolution mocks and shown to be robust and precise, with systematic errors far below the statistical thresholds. Inclusion of the bispectrum yields consistent parameter constraints and shrinks the σ_8 posterior by 13% to reach $< 5\%$ precision; less conservative analysis choices would reduce the error-bars further. Our constraints are broadly consistent with *Planck*: in particular, we find $H_0 = 69.6^{+1.1}_{-1.3}\,\mathrm{km\,s^{-1}Mpc^{-1}}$, $\sigma_8 = 0.692^{+0.035}_{-0.041}$ and $n_s = 0.870^{+0.067}_{-0.064}$, including a BBN prior on the baryon density. When n_s is set by *Planck*, we find $H_0 = 68.31^{+0.83}_{-0.86}\,\mathrm{km\,s^{-1}Mpc^{-1}}$ and $\sigma_8 = 0.722^{+0.032}_{-0.036}$. Our S_8 posterior, 0.751 ± 0.039, is consistent with weak lensing studies, but lower than *Planck*. Constraints on the higher-order bias parameters are significantly strengthened from the inclusion of the bispectrum, and we find no evidence for deviation from the dark matter halo bias relations. These results represent the most complete full-shape analysis of BOSS DR12 to-date, and the corresponding spectra will enable a variety of beyond-ΛCDM analyses, probing phenomena such as the neutrino mass and primordial non-Gaussianity.

Note: BBN prior is used

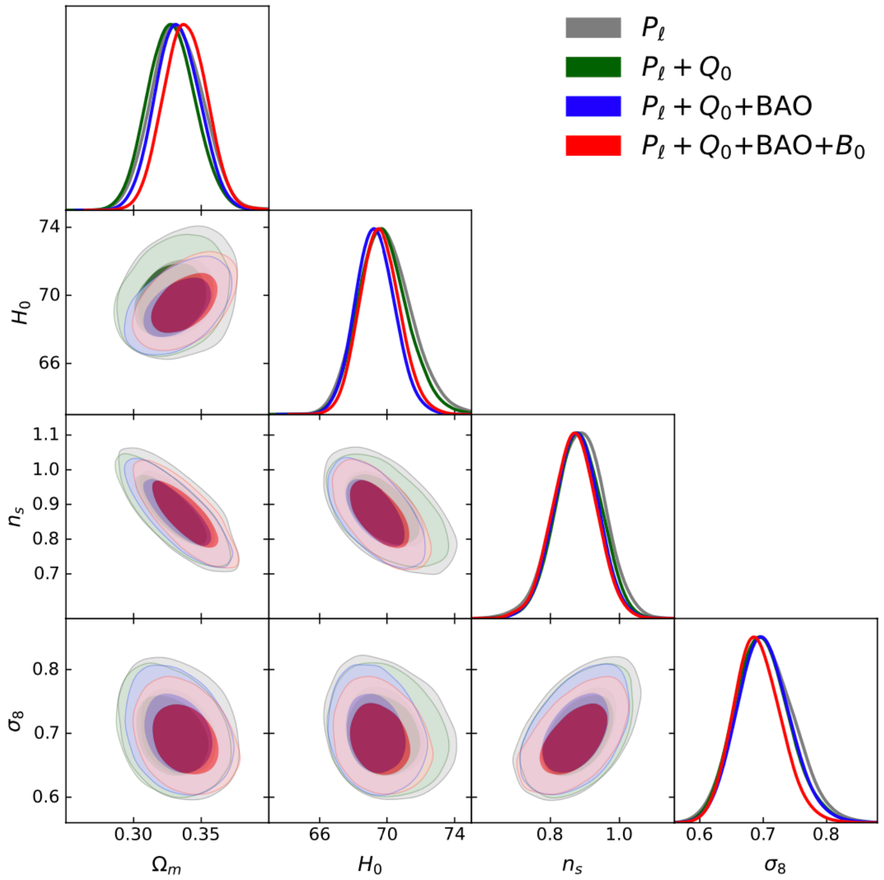

Redshift Space P0,P2,P4
+ Real Space P(k) computed from the above
+ BAO
+ Bispectrum

Theory model underneath is based on Effective Field Theory of the LSS

$$Q_0(k) \equiv P_0(k) - \tfrac{1}{2}P_2(k) + \tfrac{3}{8}P_4(k)$$

The S8 tension

$$S_8 \equiv \sigma_8 \left(\Omega_m/0.3\right)^{0.5}$$

$S_8^{Planck} = 0.832 \pm 0.012$ CMB

$S_8^{\mathrm{DES}} = 0.776 \pm 0.017$ DES (Weak lensing and clustering)

$S_8 = 0.734^{+0.035}_{-0.041}$ Galaxy Clustering Full Shape

Agreement with WL and 2.5sigma tension with CMB!

Effective field theory of LSS

$$\frac{Df}{Dt} = \frac{\partial f}{\partial t} + \frac{1}{m}\boldsymbol{p}\cdot\nabla f - m\nabla\Phi\cdot\frac{\partial f}{\partial \boldsymbol{p}} = 0$$ VLASOV EQ.

1) Start from Vlasov
2) Filter Vlasov and define IR and UV regimes
3) Small scales "backreact" on Large Scales with an effective pressure

$$\begin{aligned} m\int_{\boldsymbol{p}} f(\boldsymbol{x},\boldsymbol{p},\eta) &\equiv \rho_m(\boldsymbol{x},t)\,, \\ m\int_{\boldsymbol{p}} \frac{p_i}{m} f(\boldsymbol{x},\boldsymbol{p},t) &\equiv \rho_m v_i(\boldsymbol{x},t)\,, \\ m\int_{\boldsymbol{p}} \frac{p_i p_j}{m^2} f(\boldsymbol{x},\boldsymbol{p},t) &\equiv \rho_m v_i v_j(\boldsymbol{x},t) + \kappa_{ij}(\boldsymbol{x},t)\,. \end{aligned}$$

Moments of f
to define density
velocity and stress energy tensor

$$\partial_t\rho_m + \nabla_i(\rho_m v^i) = 0\,.$$ Continuity

$$\rho_m\left[\dot{v}^i + v^j\nabla_j v^i\right] + \rho_m\nabla_i\Phi = 0\,.$$ Euler

Ansatz for a generic fluid with viscosity

$$\kappa_{ij} = -p\delta_{ij} + \eta\left[\nabla_i v_j + \nabla_j u_i - \frac{2}{3}\delta_{ij}\nabla\cdot\boldsymbol{v}\right] + \zeta\delta_{ij}\nabla\cdot\boldsymbol{v}$$

NOW: separate the scales between long modes (l) and short modes (s)

$$3p_{\rm eff} = [\tau^k_{\ k}]_\Lambda = [\rho v^s_k v^s_k]_\Lambda - \frac{[\phi^s_{,k}\phi^s_{,k}]_\Lambda}{8\pi G}\,.$$

$$\rho_{\rm eff} = [\gamma(v_s)\rho_m]_\Lambda + \frac{1}{2}[\rho_m\phi^s]_\Lambda\,, \qquad \rho_m \equiv \gamma(v_s)e^{-3\phi_s}\rho\,, \qquad \gamma(v_s) \equiv \frac{1}{\sqrt{1-v_s^2}}\,,$$

$$\rho_{\rm eff} = \left[\rho_m\left(1 + \frac{1}{2}v_s^2 + \frac{1}{2}\phi_s\right)\right]_\Lambda\,,$$

Effective energy densities gets velocity and gravitational correction and can be derived in full GR as well

$$\rho_\ell\left[\dot{v}^i_\ell + v^j_\ell\nabla_j v^i_\ell\right] + \rho_\ell\nabla_i\phi_\ell = -\nabla_j\left[\tau^j_{\ i}\right]_\Lambda\,,$$ [...] Lambda is spatial average over 1/Lambda scale

$$\tau^i_{\ j} \equiv \rho_m v^s_i v^s_j - \frac{\phi^s_{,k}\phi^s_{,k}\delta_{ij} - 2\phi^s_{,i}\phi^s_{,j}}{8\pi G}\,.$$

Effective stress tensor in Euler eq. induced by small scale fluctuations

Note validity range: $\dfrac{k}{k_{\rm NL}} \ll 1$

$$(2\pi^2)^{-1}P_{\rm lin}(k_{\rm NL})k^3_{\rm NL} \approx 1\,.$$

$k^{-1}_{\rm NL} \sim 5$ Mpc

Effective field theory of LSS - II

Now the problem is to calculate the effective stress tensor

$$\frac{1}{a\rho}\partial_j \tau^{ij} = \int d\tau' \; K(\tau,\tau') \; \partial^i \delta(\mathbf{x}_{\rm fl}[\mathbf{x},\tau;\tau'],\tau') + \dots ,$$

Time propagator Fluid element

Taylor expand the above

$$-\frac{1}{a\rho}\partial_j \tau^{ij} = -c_s^2 \partial^i \delta + \frac{c_v^2}{\mathcal{H}} \partial^i \partial_k v^k - c_1 \partial^i \delta^2 - c_2 \partial^i (s^{kl} s_{kl}) - c_3 s^{ij} \partial_j \delta - \frac{1}{a\rho}\partial_j \tau^{ij}_{\rm stoch.}$$

Insert the above in Euler equation --> and compute!
Convenient to set the stress energy to zero first
and then look for corrections to this

$$\delta = [\delta_{(1)} + \delta_{(2)} + \delta_{(3)} + \dots] + \delta^{\rm c}_{(1)} + \dots$$

Biased tracers (e.g. galaxies, DM haloes)

$$\delta_g = b_1 \delta + \frac{b_2}{2}\delta^2 + b_{\mathcal{G}_2}\mathcal{G}_2 + b_{\nabla^2\delta}\nabla^2\delta + b_{\Gamma_3}\Gamma_3 + \varepsilon + \dots$$

$$\mathcal{G}_2(\Phi) \equiv (\partial_i\partial_j\Phi)^2 - (\Delta\Phi)^2 , \quad \Gamma_3 \equiv \mathcal{G}_2(\Phi) - \mathcal{G}_2(\Phi_v)$$

+ redshift space distortions...
+ baryons....
+ neutrinos....

$$\delta^{\rm ctr.} = -c_0 \left(\frac{k}{k_{\rm NL}}\right)^2 - (c_1\mu^2 + c_2\mu^4)\left(\frac{k}{k^r_{\rm NL}}\right)^2$$

modelling of Fingers of God

Things get non-trivial with many parameters... but...

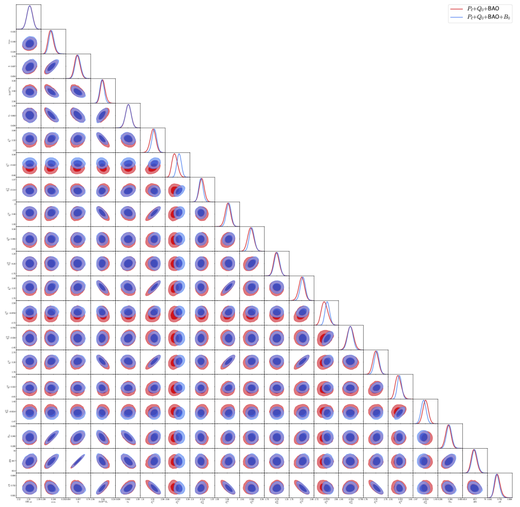

from BOSS DR12

Future seems bright

DESI paper (2016) - stage IV experiment - Y1 DR in Fall 2023 / early data release in Jan 23

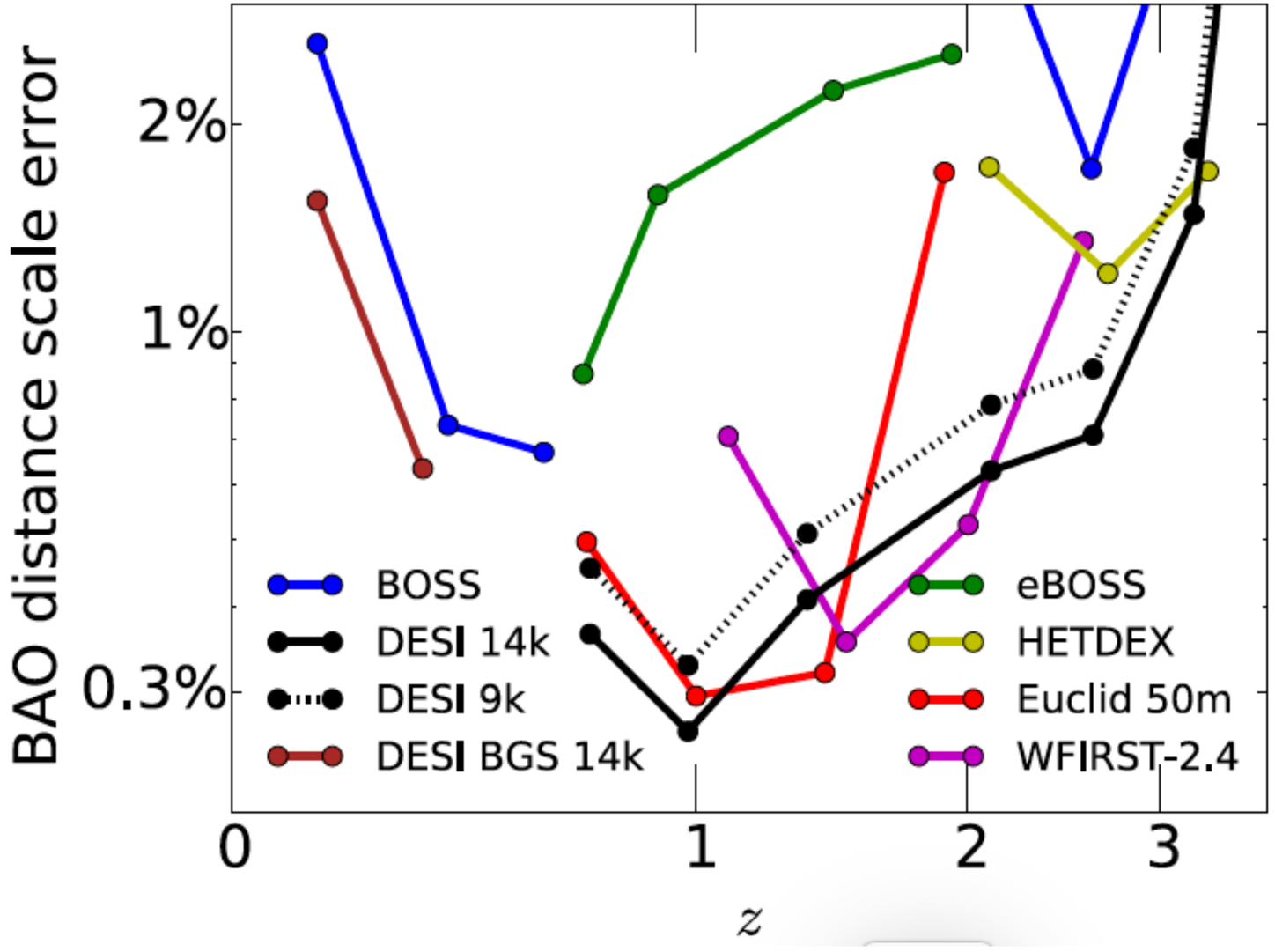

"Conclusions"

Future galaxy redshift surveys (e.g. DESI from the ground or Euclid from the sky) will continue an on-going effort to map the large-scale galaxy distribution

Different features of the galaxy power spectrum provide different constraint on the cosmological model:

- **BAO are a standard ruler, a geometrical probe of the expansion history**
- **The anisotropy of the galaxy power spectrum (Redshift-Space Distortions) measure instead the growth of structure**
- **The "shape" of the power spectrum provide an upper bound on neutrino masses**

Current efforts are aimed at extracting all available information in 2-point and higher-order correlation functions and extend PT predictions beyond the Standard Cosmological Model ---> Bispectrum/ Trispectrum.... etc

Challenges of GC studies for dark energy

- bias modelling at mildly non-linear scales to exlpoit also other smaller volume surveys

- neutrino mass measurement and modelling of neutrino induced non-linearities in GCs (scale dependence of the bias)

- higher order statistics and the search for non-Gaussianities

- Cross correlations

- Multi purpose experiments with high degree of complementarity

- Machine learning and data science (pixel-by-pixel analysis)

- **High redshift regime/huge discovery potential**

Ultimate error achievable on the power spectrum (maximum amount of information in the sky)

Cosmic Visions Dark Energy 2016

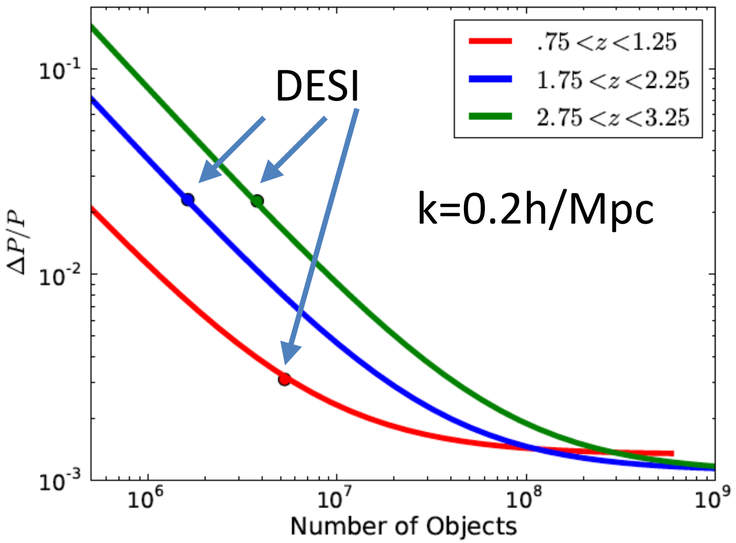

Euclid

Euclid definition study report 2011

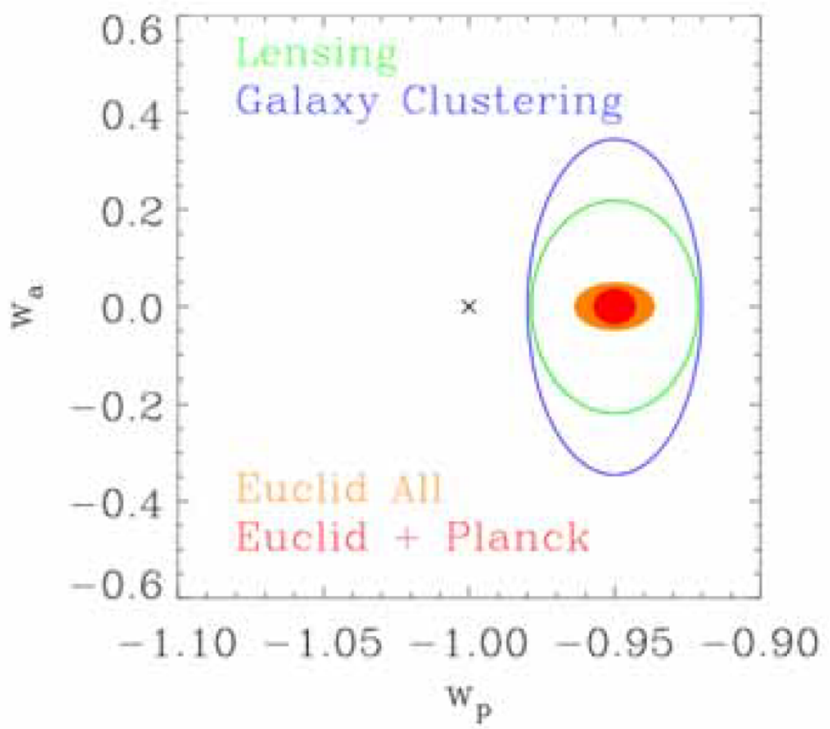

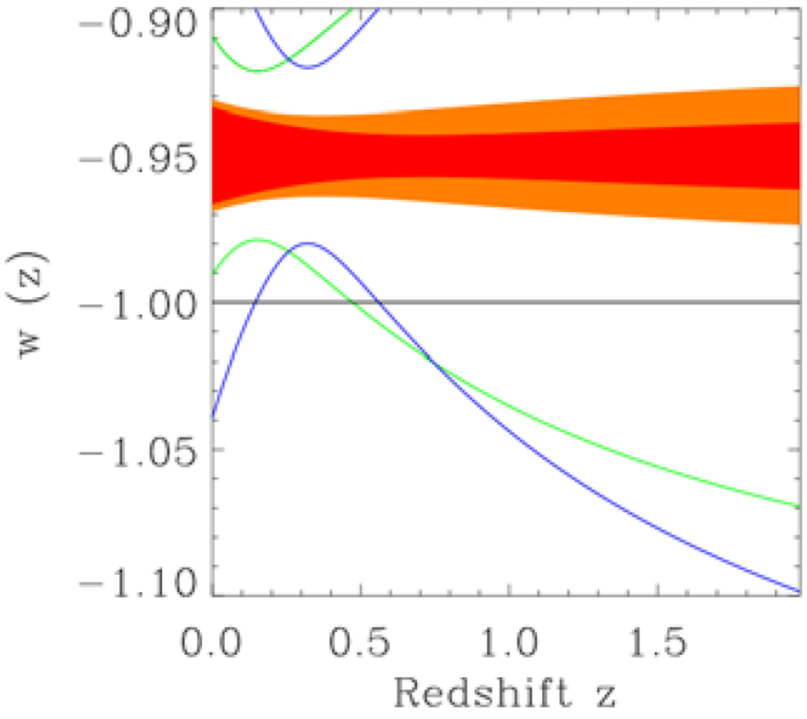

GC+WL

GC+WL+GCs+ISW

	Dark Energy		
Parameter	w_p	w_a	*FoM*
Euclid Primary	0.015	0.150	430
Euclid All	0.013	0.048	1540
Euclid+Planck	0.007	0.035	4020
Current	0.100	1.500	~10
Improvement Factor	**>10**	**>50**	**>300**

DESI constraints

Table 2.9: DETF Figures of Merit and uncertainties σ_{w_p} and σ_{Ω_k}. σ_{w_p} is the error on w at the pivot redshift, which also equal to the error on a constant w holding $w_a = 0$. σ_{Ω_k} is the error on the curvature of the Universe, Ω_k. All DESI lines contain the BGS, and BOSS in the range $0.45 < z < 0.6$ that does not substantially overlap with DESI. All cases include *Planck* CMB constraints. The pivot point, where $w(a)$ has minimal uncertainty is indicated by a_p. We note that a FoM of 110 is 10 times the Stage II level of [109], which we take to be the definition of Stage IV. DESI BAO galaxy exceeds this threshold even with a 9,000 square degree survey.

Surveys	FoM	a_p	σ_{w_p}	σ_{Ω_k}
BOSS BAO	37	0.65	0.055	0.0026
DESI 14k galaxy BAO	133	0.69	0.023	0.0013
DESI 14k galaxy and Ly-α forest BAO	169	0.71	0.022	0.0011
DESI 14k BAO + gal. broadband to $k < 0.1\ h$ Mpc^{-1}	332	0.74	0.015	0.0009
DESI 14k BAO + gal. broadband to $k < 0.2\ h$ Mpc^{-1}	704	0.73	0.011	0.0007
DESI 9k galaxy BAO	95	0.69	0.027	0.0015
DESI 9k galaxy and Ly-α forest BAO	121	0.71	0.026	0.0012
DESI 9k BAO + gal. broadband to $k < 0.1\ h$ Mpc^{-1}	229	0.73	0.018	0.0011
DESI 9k BAO + gal. broadband to $k < 0.2\ h$ Mpc^{-1}	502	0.73	0.013	0.0009

Dark Energy after Planck - I

Planck Paper XIV "Dark Energy and Modified Gravity" (2016)

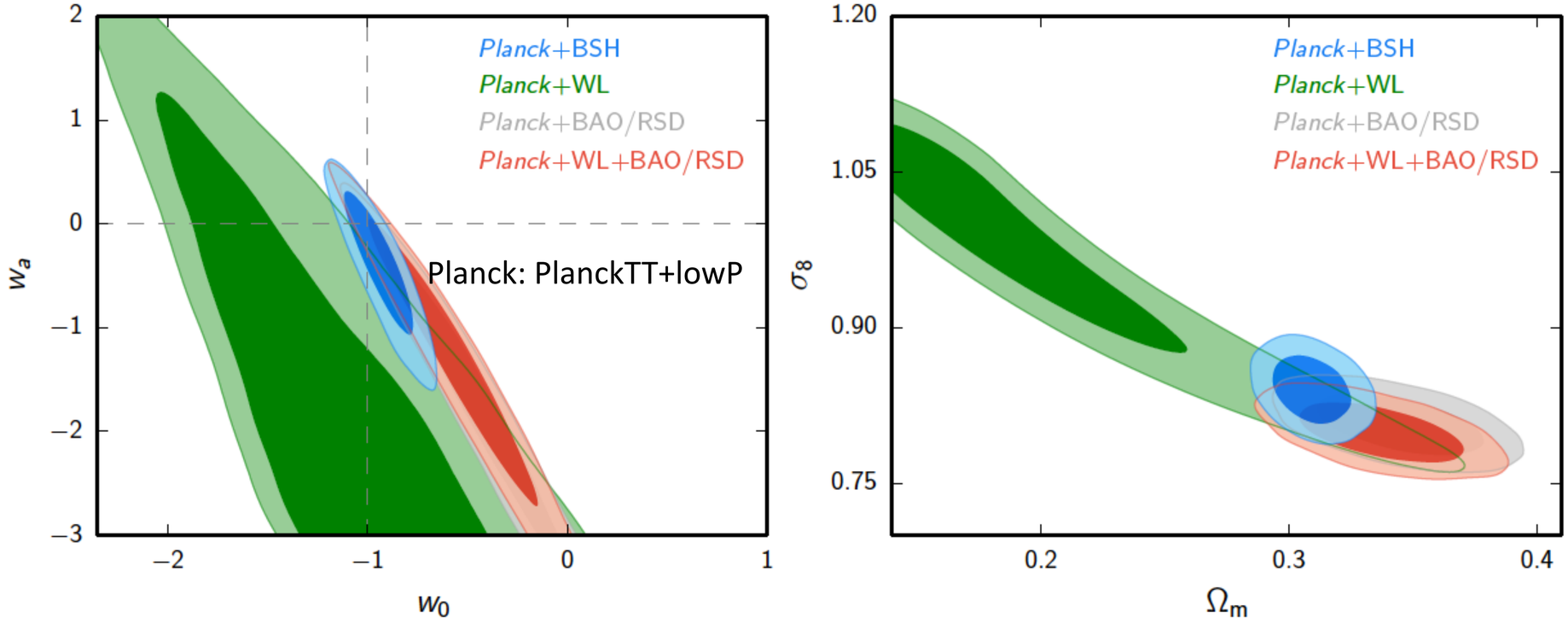

Planck+BSH combination has a $\Delta\chi^2$=-0.8 w.r.t. base LCDM

WL is CFHTLens: prefers w_0-w_a at 2σ w.r.t. LCDM, wants higher σ_8 and (not show
value of H_0

Implications for the small scale crisis of LCDM

Dark Energy after Planck - II

Planck Paper XIV

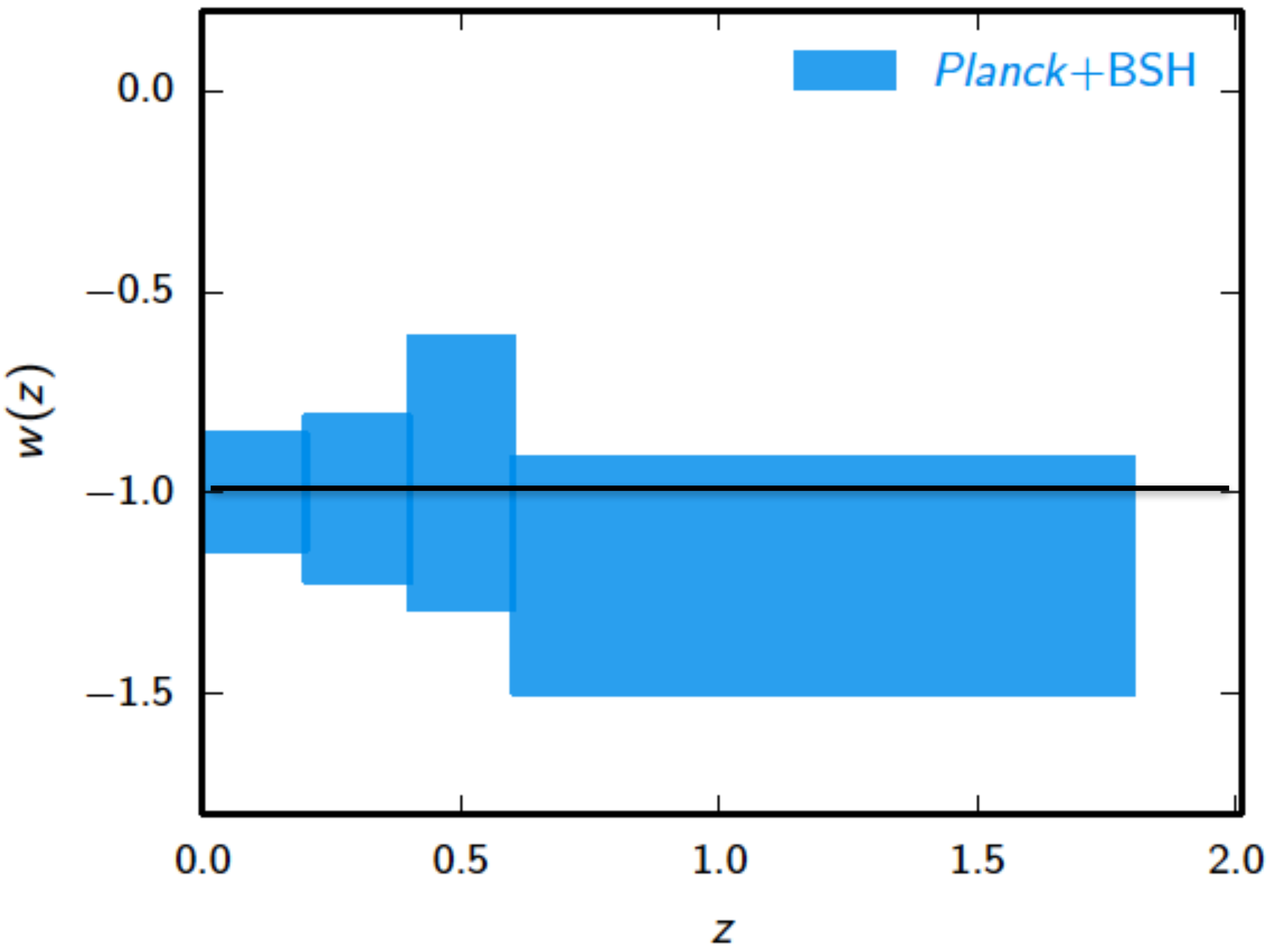

Principal Component Analysis reconstruction in 4 bins, increasing number of bins does lead to same conclusions.

$$w(z) = p_{i-1} + \Delta w \left(\tanh \left[\frac{z - z_i}{s} \right] + 1 \right) \text{ for } z < z_i, \ \text{i} \in \{1, 4\}$$

Dark Energy after Planck - III

Planck Paper XIV

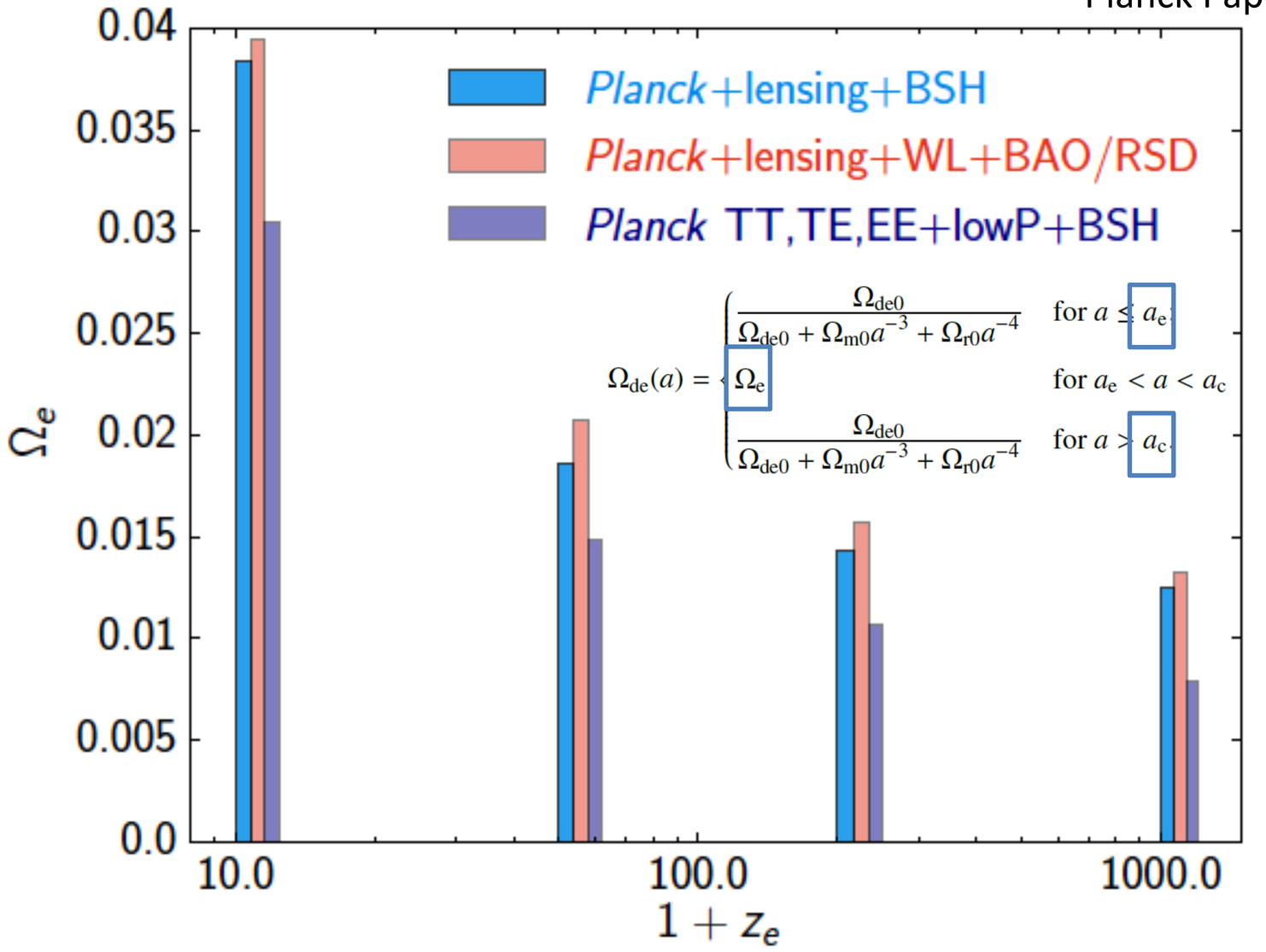

Note further that Planck is providing a measurement of the sound horizon at the drag epoch with an error of 0.2% …

Dark Energy after Planck - IV

Remarkable results from Planck experiment in constraining DE properties

1) In (w_0-w_a), Planck TT+lowP+BSH is compatible with LCDM, as well as BAO/RSD. When adding WL to Planck TT+lowP, both WL and CMB prefer the (w_0-w_a) model with respect to LCDM at ~2σ (with preference for high values of H_0, excluded when including BSH). CMB lensing does not change the numbers.

2) Tests on time varying w(z) are compatible with LCDM for all data sets tested.

3) EDE model with constant fraction till recent. Constraints are incredibly tight: previous constraints improved by a factor 3-4, Ω_e <0.0036 for PlanckTT,TE,EE+lowP+BSH. Polarization improves limits by a factor 2.

4) $\Omega_e(z)$ as a function of z_e , the redshift starting from which a fraction is present. Ω_e < 2% (95% C.L.) even for z_e as late as 50 (important results in the era of **structure formation** with implications for EDGES and other science). CMB lensing is important.

Lyman-alpha BAO: a tuned oscillation?

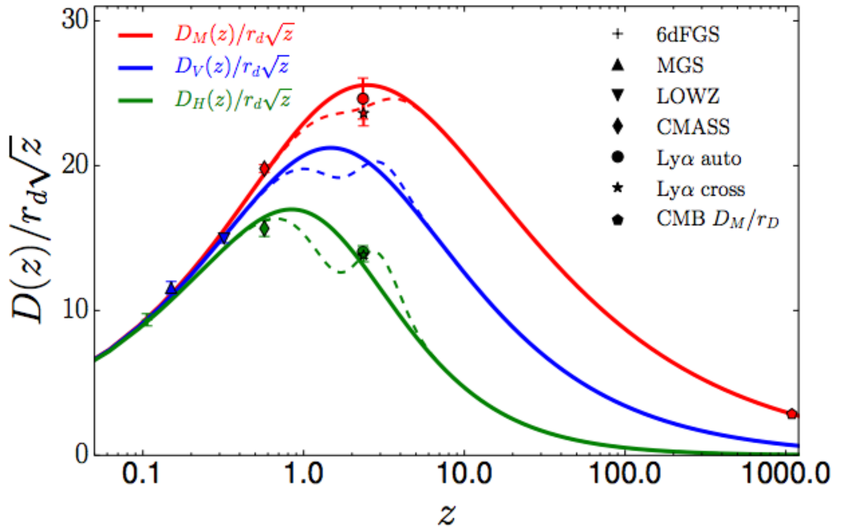

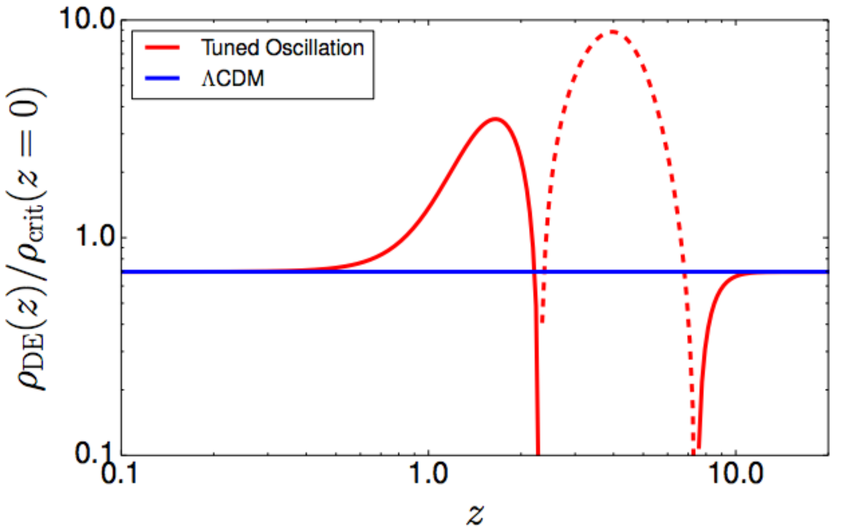

$\Delta\chi^2$=-6.6 with 3 d.o.f. for this model

Dark Energy Experiments: 2013 - 2031

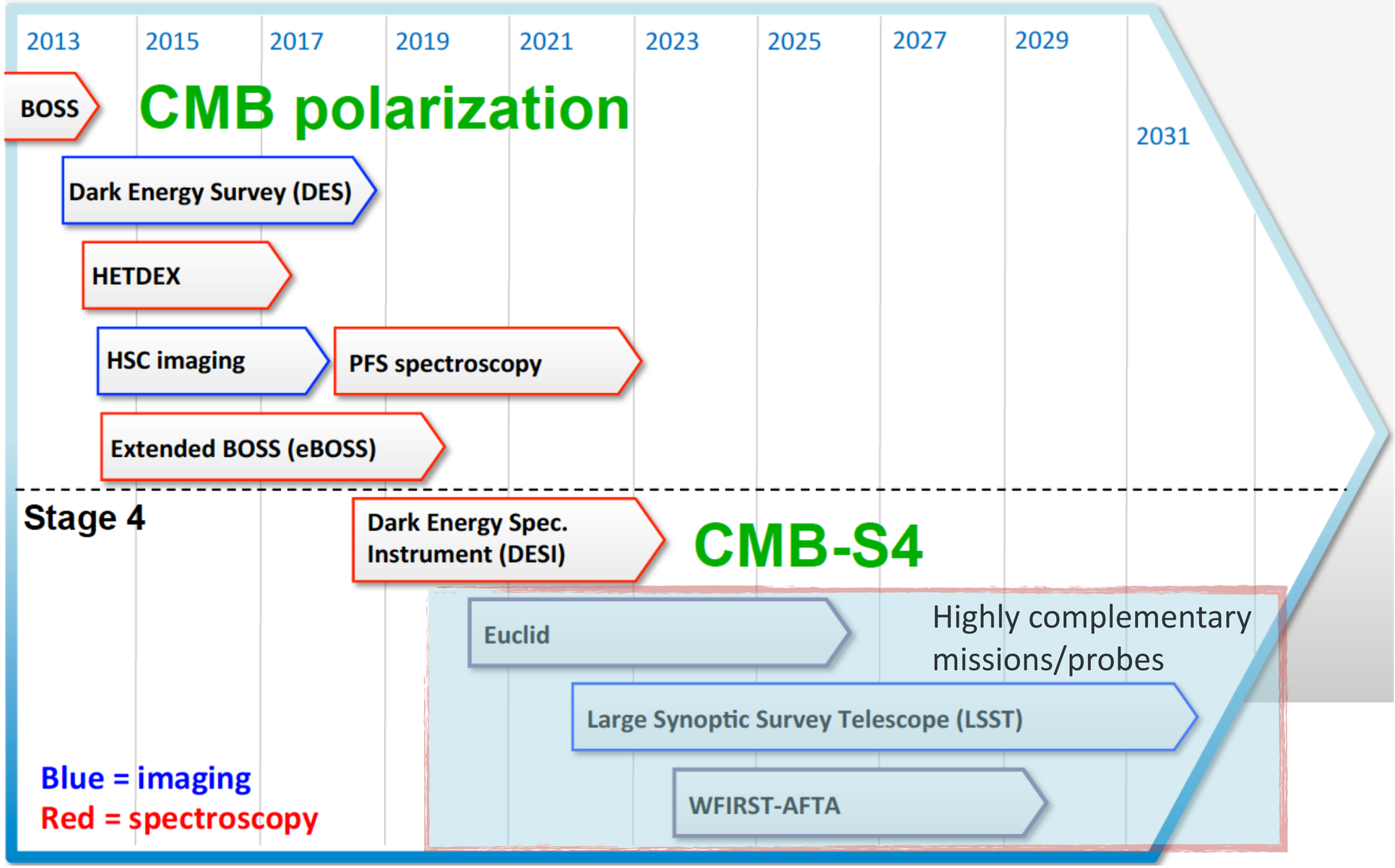

SDSS/BOSS-IV: cosmological implications

Bautista+ 17, arXiv: 1702.00176

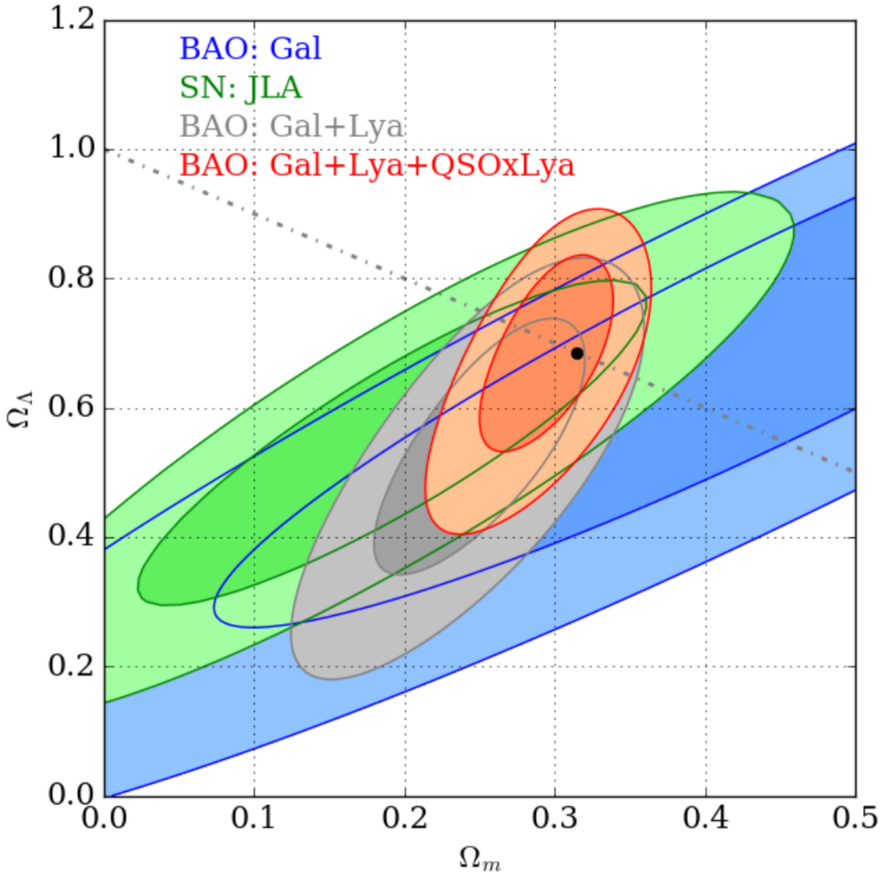

- Redshift covered z=2.1-3.5, <z>=2.33.
- 160,000 QSOs (DESI will have ~ 10 times more.
- Statistical improvement over DR9, DR11 (Delubac+14) hinted for a change in the sign of dark energy density to reconcile with Planck.
- Better physical modelling for high column density systems, UV fluctuations, broad band power (marginalized over).
- Complementarity with low redshift BAO, high redshift BAO provide a stronger support for $\Omega_\Lambda > 0$ (independent of CMB).

$$\Omega_M = 0.296 \pm 0.029 \qquad \Omega_\Lambda = 0.699 \pm 0.100$$

$$\Omega_k = -0.002 \pm 0.119$$

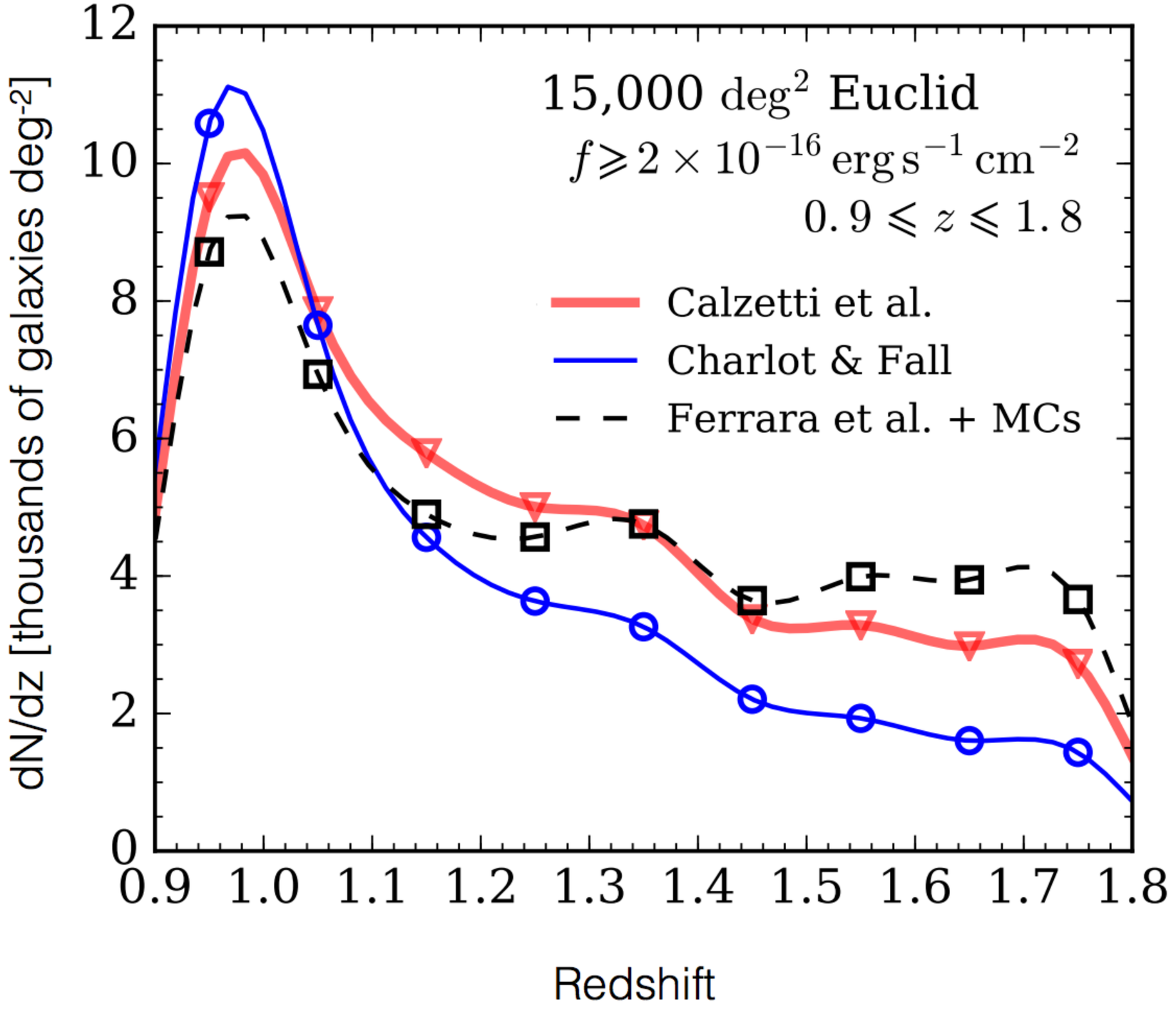
15,000 deg^2 Euclid
$f \geqslant 2 \times 10^{-16}\,\mathrm{erg\,s^{-1}\,cm^{-2}}$
$0.9 \leqslant z \leqslant 1.8$
Calzetti et al.
Charlot & Fall
Ferrara et al. + MCs
dN/dz [thousands of galaxies deg^{-2}]
Redshift
0
2
4
6
8
10
12
0.9
1.0
1.1
1.2
1.3
1.4
1.5
1.6
1.7
1.8